

2

NAVAL POSTGRADUATE SCHOOL

Monterey, California

AD A113848



DTIC
ELECTE
APR 26 1982
S B

THESIS

POWER SPECTRA OF GEOMAGNETIC FLUCTUATIONS
BETWEEN 0.02 and 10 Hz

by

Michael Wayne Beard

December 1981

Thesis Advisor:

P. Moose

Approved for public release; distribution unlimited

SHIP FILE COPY

82 04 24 083

Unclassified

SECURITY CLASSIFICATION OF THIS PAGE (When Data Entered)

REPORT DOCUMENTATION PAGE		READ INSTRUCTIONS BEFORE COMPLETING FORM
1. REPORT NUMBER	2. GOVT ACCESSION NO.	3. RECIPIENT'S CATALOG NUMBER
	HD 4113848	
4. TITLE (and Subtitle)		5. TYPE OF REPORT & PERIOD COVERED
Power Spectra of Geomagnetic Fluctuations Between 0.02 and 20 Hz		Master's Thesis December 1981
6. AUTHOR(s)		7. PERFORMING ORG. REPORT NUMBER
Michael Wayne Beard		
8. PERFORMING ORGANIZATION NAME AND ADDRESS		9. CONTRACT OR GRANT NUMBER(s)
Naval Postgraduate School Monterey, California 93940		
10. CONTROLLING OFFICE NAME AND ADDRESS		11. PROGRAM ELEMENT, PROJECT, TASK AREA & WORK UNIT NUMBERS
Naval Postgraduate School Monterey, California 93940		
12. MONITORING AGENCY NAME & ADDRESS (if different from Controlling Office)		13. REPORT DATE
		December 1981
		14. NUMBER OF PAGES
		110
		15. SECURITY CLASS. (of this report)
		Unclassified
		16a. DECLASSIFICATION/DOWNGRADING SCHEDULE
17. DISTRIBUTION STATEMENT (of this Report)		
Approved for public release; distribution unlimited		
18. DISTRIBUTION STATEMENT (of the abstract entered in Block 20, if different from Report)		
19. SUPPLEMENTARY NOTES		
20. KEY WORDS (Continue on reverse side if necessary and identify by block number)		
Geomagnetic Power Spectra, .02-20 Hz, Pcl, EAST-WEST Component. Solar Powered Telemetry, Schumann Resonance Peak Splitting, Concurrent Land-Underwater Data		
21. ABSTRACT (Continue on reverse side if necessary and identify by block number)		
<p>Fluctuations of the East-West component of the Earth's geomagnetic field were measured at a remote land site. The resulting data were transmitted by a solar powered telemetry system to the Naval Postgraduate School at Monterey, California, and the power spectra for the frequency range of .02-20 Hz calculated. The measurements, which covered a 4-month interval (July 20 - October 10, 1981), consistently show a minimum of activity in the interval 3-7 Hz. (Continued)</p>		

DD FORM 1473

EDITION OF 1 NOV 68 IS OBSOLETE
S/N 0103-016-0601

Unclassified

SECURITY CLASSIFICATION OF THIS PAGE (When Data Entered)

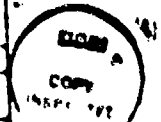
Unclassified

SECURITY CLASSIFICATION OF THIS PAGE/When Data Entered

Item 20. (Continued)

At frequencies below the minimum, in the range of .02 - 3 Hz, the typical monotonic decrease in background activity with frequency was observed. At 1 Hz an average power spectral density of 1×10^{-2} nT²/Hz was observed during the day and 3.1×10^{-3} nT²/Hz at night. In contrast, at frequencies above the minimum, in the range 7-14 Hz, the activity is dominated by the first Schumann resonance. An evaluation of the East-West component spectra and concurrent underwater horizontal component measurements showed a 90% correlation with the underwater spectra. The underwater field strengths were normally 3-5 dB less than the strengths measured on land. Splitting of the first Schumann resonance peak into a doublet structure was observed in 10% of the land data.

Accession For	
NTIS GRA&I	<input checked="" type="checkbox"/>
DTIC TAB	<input type="checkbox"/>
Unannounced	<input type="checkbox"/>
Justification	
By	
Distribution/	
Availability Codes	
Avail and/or	
Dist	Special
A	



Unclassified

SECURITY CLASSIFICATION OF THIS PAGE/When Data Entered

Approved for public release; distribution unlimited

Power Spectra of Geomagnetic Fluctuations
Between 0.02 and 20 Hz

by

Michael Wayne Beard
Captain, U.S. Army
B.S., United States Military Academy, 1971

Submitted in partial fulfillment of the
requirements for the degree of

MASTER OF SCIENCE IN PHYSICS

from the

NAVAL POSTGRADUATE SCHOOL

December 1981

Author:

Michael Wayne Beard

Approved by:

John J. ...

Thesis Advisor

Otto Heuz

Second Reader

John J. ...
Chairman, Department of Physics & Chemistry

William M. ...

Dean of Science and Engineering

ABSTRACT

Fluctuations of the East-West component of the Earth's geomagnetic field were measured at a remote land site. The resulting data were transmitted by a solar powered telemetry system to the Naval Postgraduate School at Monterey, California. and the power spectra for the frequency range of .02 - 20 Hz calculated. The measurements, which covered a 4-month interval (July 20 - October 10, 1981), consistently show a minimum of activity in the interval 3 - 7 Hz. At frequencies below the minimum, in the range of .02 - 3 Hz, the typical monotonic decrease in background activity with frequency was observed. At 1 Hz an average power spectral density of 1×10^{-2} nT²/Hz was observed during the day and 3.1×10^{-3} nT²/Hz at night. In contrast, at frequencies above the minimum, in the range 7-14 Hz, the activity is dominated by the first Schumann resonance. An evaluation of the East-West component spectra and concurrent underwater horizontal component measurements showed a 90% correlation with the underwater spectra. The underwater field strengths were normally 3-5 dB less than the strengths measured on land. Splitting of the first Schumann resonance peak into a doublet structure was observed in 10% of the land data.

TABLE OF CONTENTS

I.	INTRODUCTION	9
II.	BACKGROUND	10
	A. MAIN MAGNETIC FIELD	10
	B. ELEMENTS OF THE FIELD	11
	C. TIME VARIATIONS OF THE FIELD	12
	D. PREVIOUS WORK	17
III.	SYSTEM DESCRIPTION	19
	A. REMOTE MONITORING SITE	19
	B. SYSTEM COMPONENTS	21
	C. SYSTEM TRANSFER FUNCTION	25
	D. SYSTEM NOISE	27
IV.	EXPERIMENTAL RESULTS	31
	A. INTRODUCTION	31
	B. REVIEW OF DATA	32
	C. OBSERVATIONS AND RECOMMENDATIONS	55
V.	EQUIPMENT/SYSTEM IMPROVEMENTS AND RECOMMENDATIONS --	57
	APPENDIX A. EXPERIMENTAL EQUIPMENT AND TESTS	60
	APPENDIX B. SYSTEM CALIBRATION	73
	APPENDIX C. EQUIPMENT SCHEMATICS	79
	APPENDIX D. EQUIPMENT USAGE AND MAINTENANCE	82
	APPENDIX E. COMPUTER PROGRAMS	92
	BIBLIOGRAPHY	108
	INITIAL DISTRIBUTION LIST	109

<u>Figure</u>	<u>LIST OF FIGURES</u>	<u>Page</u>
1.	Dipole Appearance of the Geomagnetic Field -----	10
2.	Elements of the Field -----	11
3.	Power Spectrum of Geomagnetic Disturbances Observed on the Surface of the Earth -----	16
4.	Chew's Ridge Site Location -----	20
5.	Data Collection System -----	22
6.	Data Processing System -----	23
7.	Radio Power Supply -----	24
8.	System Transfer Function -----	26
9.	Preamplifier Noise Comparison -----	29
10.	System Noise -----	30
11.	Chew's Ridge Sensor Orientation -----	33
12.	East-West Magnetic Field Fluctuations (.01-5 Hz) 8/21/81, 1345 Hrs. -----	36
13.	East-West Magnetic Field Fluctuations (.1-20 Hz) 8/21/81, 1345 Hrs. -----	37
14.	East-West Magnetic Field Fluctuations (.01-5 Hz) 8/24/81, 1935 Hrs. -----	38
15.	East-West Magnetic Field Fluctuations (.1-20 Hz) 8/24/81, 1935 Hrs. -----	39
16.	East-West Magnetic Field Fluctuations (.01-5 Hz) 8/25/81, 0045 Hrs. -----	40
17.	East-West Magnetic Field Fluctuations (.1-20 Hz) 8/25/81, 0045 Hrs. -----	41
18.	East-West Magnetic Field Fluctuations (.01-5 Hz) 8/25/81, 0618 Hrs. -----	42
19.	East-West Magnetic Field Fluctuations (.1-20 Hz) 8/25/81, 0618 Hrs. -----	43

20.	East-West Magnetic Field Fluctuations (.01-5 Hz) 10/04/80, 1130 Hrs. -----	45
21.	East-West Magnetic Field Fluctuations (.1-20 Hz) 10/04/81, 1135 Hrs. -----	46
22.	East-West Magnetic Field Fluctuations (.01-5 Hz) 10/04/81, 1855 Hrs. -----	47
23.	East-West Magnetic Field Fluctuations (.1-20 Hz) 10/04/81, 1855 Hrs. -----	48
24.	East-West Magnetic Field Fluctuations (.01-5 Hz) 10/04/81, 2330 Hrs. -----	49
25.	East-West Magnetic Field Fluctuations (.1-20 Hz) 10/04/81, 2330 Hrs. -----	50
26.	East-West Magnetic Field Fluctuations (.01-5 Hz) 10/05/81, 0830 Hrs. -----	51
27.	East-West Magnetic Field Fluctuations (.1-20 Hz) 10/05/81, 0830 Hrs. -----	52
28.	Average Day and Night Power Spectral Density: August-October, 1981 -----	54
29.	Amplifier Gain Characteristics -----	62
30.	VCO/FTV Gain Characteristics -----	65
31.	Theoretical Sensor Sensitivity -----	77
32.	Schematic of the Preamplifier Circuit -----	80
33.	Schematic of the Voltage-Controlled Oscillator Circuit -----	81

ACKNOWLEDGEMENT

Although many people contributed directly and indirectly to this thesis, I owe a special thanks to Dr. Paul Moose and Dr. Otto Heinz, my advisors for this work. I am sincerely grateful for their guidance and assistance.

I am also deeply indebted to Mr. Robert Smith and Mr. William Smith of the Electrical Engineering Department for their technical expertise, knowledge, and skill in overcoming the problems associated with electrical interconnections. For this, and the many long hours working on Chew's Ridge, I offer my sincere thanks.

Finally, I would like to thank my wife, Sharyn, for putting up with the long hours, carrying heavy equipment up mountain ridges on hot days and converting my illegible scratchings into a readable manuscript.

I. INTRODUCTION

This thesis research is part of an ongoing effort at the Naval Postgraduate School to obtain improved long-term data and interpretations of the electromagnetic noise on the ocean floor. The project objective is to study and interpret signals in the frequency range from .01 Hz to 100 Hz. The overall project emphasizes the importance of obtaining measurements of geomagnetic noise fluctuations on the sea floor and on land over a period of several years.

The particular objectives of this thesis are:

1. To install a remote land-based monitoring site and a telemetry system for the transmission of geomagnetic data to the Naval Postgraduate School.
2. To collect the east-west component of the local magnetic field fluctuation data for comparison with sea floor data and to test the system's sensitivity.

II. BACKGROUND

A. MAIN MAGNETIC FIELD

World magnetic surveys at ground level and, more recently, by satellite indicate that the principal source of the main geomagnetic field is beneath the earth's crust. Approximately 90% of the main field exhibits characteristics roughly equivalent to the field of a terrestrial-centered short bar magnet or dipole inclined at 11.5° to the axis of rotation.

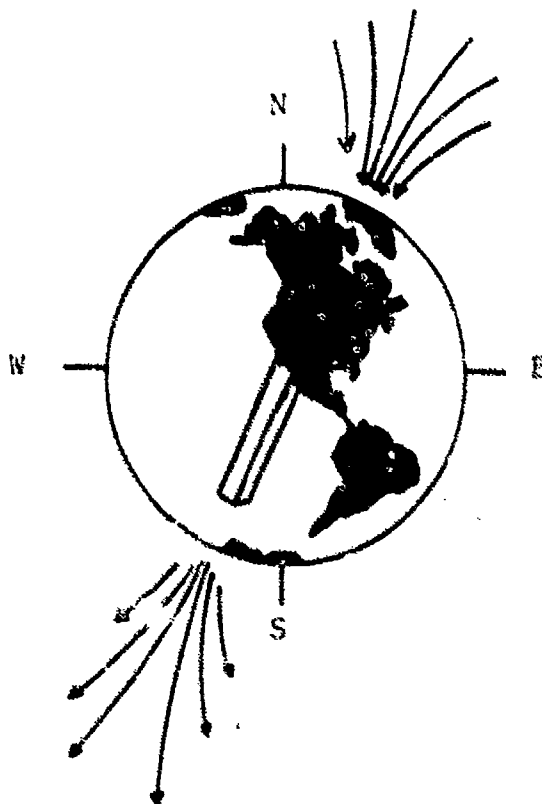


Figure 1. Dipole Appearance on Geomagnetic Field

B. ELEMENTS OF THE FIELD

The various components of the magnetic field are shown in Figure 2. They are defined as:

X = North-South Component

Y = East-West Component

Z = Vertical Component

D = Declination Angle

H = Horizontal Component

F = Total Field

I = Inclination or Dip Angle

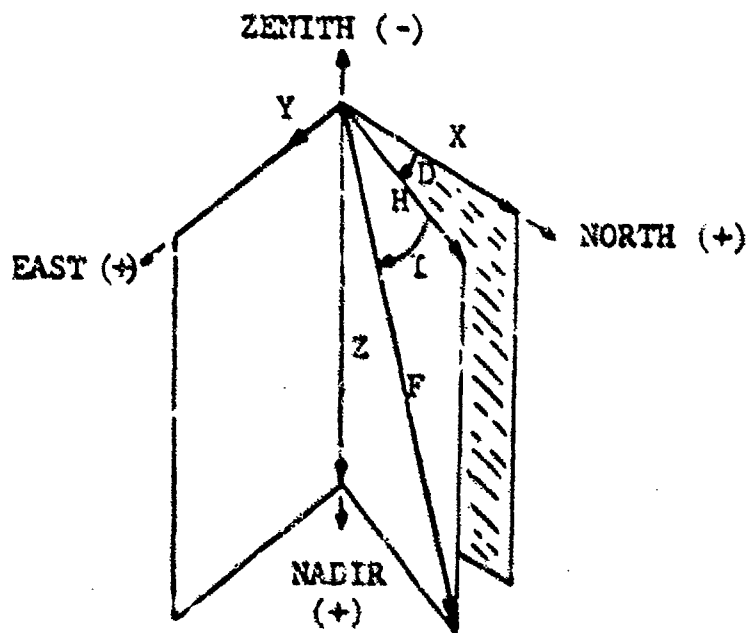


Figure 2. Elements of the Field

In terms of the familiar bar magnet, a magnet perfectly free to turn in any direction would show the direction of the field. Since it is almost impossible to suspend a single magnet in this manner, two are used: one with a vertical axis (compass) and one with a horizontal axis (dip needle). The compass shows the direction of the horizontal component H ; and when properly oriented, the dip needle shows the inclination or dip.

C. TIME VARIATIONS OF THE FIELD

The time variations of the geomagnetic field can be broadly categorized into "quiet variation fields", "disturbed variation fields", and "micropulsations".

1. Quiet Variation Field

Smoothed geomagnetic records show a consistent trend that clearly indicates a pattern of daily variation with respect to solar local time. The average variation patterns derived from chosen quiet day records define a variation field called the SOLAR QUIET DAILY VARIATION which is denoted Sq . There is also a lunar daily variation, denoted L , but it is much weaker ($L < 0.1 Sq$.) and more variable.

Two thirds of these daily (diurnal) fluctuations, i.e., those having a 24 hour period, are due to current sources external to the earth. The remaining one third is due to internal currents induced in the earth's surface layers by variable external fields. The external currents

responsible are found to flow at an approximate altitude of 100 kilometers, and are produced by convective movement of charged particles moving across the earth's magnetic field lines. The convective motion of the particles is caused mainly by solar heating of the upper atmosphere.

Therefore, the sun produces a stationary current system in the upper atmosphere, and the earth rotates under it once a day. This mechanism, known as the Atmospheric Dynamo, starts in Monterey at about sunrise and reaches its peak about noon. S_q varies characteristically with latitude. At the equator the maximum horizontal intensity is 100 nT^1 , where at higher latitudes it is generally -25 to -50 nT . S_q is also dependent on the season and the phase of the solar cycle. In the summer and during a sunspot maximum, S_q is increased; in the winter, it is decreased.

2. Disturbed Variation Fields

Any fluctuations other than the quiet day solar and lunar variations are called magnetic disturbances. All disturbances, other than those directly attributable to a solar flare or fluctuations produced by upper atmospheric irregular motions, are caused originally by disturbed solar plasma and may therefore be generally classified as belonging to one family.

Irregular magnetic fluctuations of one-to-two hours duration are related to changes in the solar wind pressure on

¹ $\text{nT} = 10^{-9} \text{ Gauss}$

magnetosphere and associated changes in the southward component of the interplanetary field. These fluctuations are sudden impulses and magnetic bays. "Sudden Impulses" are sudden increases of several nanoteslas followed by a gradual increase or decrease in the field. This is succeeded by a return, with some small oscillations, to the normal field. These latter fluctuations usually last about one to two hours.

The term magnetic storm is reserved to apply to a relatively severe, long lasting disturbance with recognizable features. Magnetic storms are caused by plasma bursts from the sun, since a solar flare emits both X rays and plasma. The X rays precede the plasma and enter the earth's atmosphere, causing increased ionization in the sunlit atmosphere. This ionization occurs in the lower ionosphere and enhances the currents in the atmospheric dynamo thereby producing what is known as the Solar Flare Effect, a precursor to magnetic storms.

The major magnetic storm disturbances are caused by dynamic pressure changes of the solar wind. When a plasma blast from the sun arrives, it suddenly increases the solar wind pressure, compressing the magnetic field (Sudden commencement). It maintains the compression for a time, called the initial phase. When the pressure decreases with the passing of the plasma blast, the circulating currents which have been induced in the magnetosphere tend to make the field intensity "overshoot" before the currents gradually dissipate. This initiates the recovery phase back to the normal quiet field

condition. The entire magnetic storm can last from one to three days with a recovery time that may be even longer.

3. Geomagnetic Micropulsation

Field changes which occur at periods of 0.2 seconds to 10 minutes are called Micropulsations. These characteristically have amplitudes from tens of nanoteslas to a fraction of one nanotesla. Micropulsations are generally divided into two types. The terminology recommended by the International Association of Geomagnetism and Aeronomy is pc for pulsation continuous and pi for pulsation irregular. The continuous (pc) micropulsations have amplitude variations which are quasi sinusoidal. The irregular (pi) micropulsations exhibit irregularities in both frequency and amplitude. The period ranges and average amplitude for these pulsations are:

pc1	.2-5 sec	0.05 - 0.1 nT
pc2	5-10 sec	0.1 - 1 nT
pc3	10-45 sec	0.1 - 1 nT
pc4	45-150 sec	0.1 - 1 nT
pc5	150-600 sec	1-10 nT
pi1	1-40 sec	0.01 - 0.1 nT
pi2	40-150 sec	1-5 nT

Micropulsations below 3 Hz are produced mainly from wave-particle interactions in the magnetosphere. Pulsations of frequencies from 3 to 3000 Hz make up the ELF region of Figure 3. This ELF region has three principle contributors: ELF "Sferics", ELF Emissions, and Earth-Ionosphere Cavity Resonances.

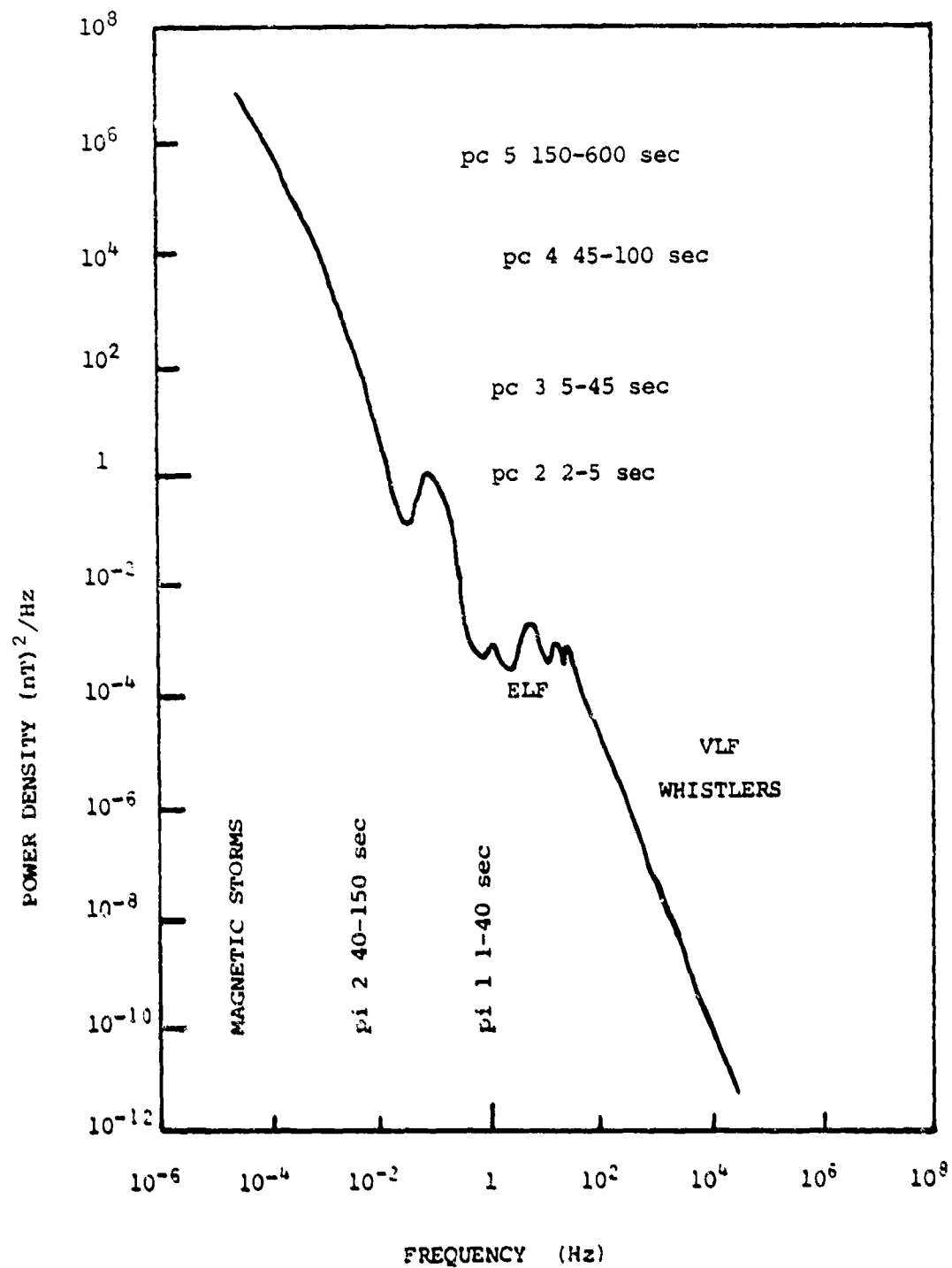


Figure 3. Power Spectrum of Geomagnetic Disturbances Observed on the Surface of the Earth
[Cladis, Davidson, and Newkirk, 1971]

ELF "Sferics" are electromagnetic signals from atmospheric electric discharges that propagate in the earth's waveguide between the ground and the lower boundary of the ionospheric E-region. The "Sferic" wave travels very long distances and its waveform consists of a main high frequency oscillatory head (VLF), followed by a lower frequency (ELF) tail-like oscillation, sometimes referred to as a "slow tail". "Sferics" commonly last about 20 milliseconds and have frequency components from 30 to several Hertz.

ELF emissions are an excitation of whistler waves (300 to 30,000 Hz), made by charged particles streaming along the earth's field lines. The whistlers in the VLF region sometimes produce lower frequency components in the ELF region.

The Cavity Resonance signals are resonantly excited by lightning transients in the concentric spherical cavity between the earth's surface and the lower region of the ionosphere. The power spectra of the signals show maxima near 7.8, 14.1, 20.3, 26.4 and 32.5 Hertz.

D. PREVIOUS WORK

Previous work by Santirocco and Parker (1963) and Park (1964) indicates that the geomagnetic field decreases with a slope of approximately -6 dB/octave between 10^{-4} and 1 Hz. From 1 to 40 Hz, the field exhibits a levelling off and is dominated by the Schumann Resonances (Schumann and Konig, 1954).

Recent measurements in the frequency range of 0.1-14 Hz were conducted by A. C. Fraser-Smith and J. L. Buxton (1975). Their measurements were taken over a two month interval at Stanford, California which is 100 km from the site used in this work. They found that the general decline in the slope (-6 dB/octave) continued to approximately 5 Hz, where the decline was arrested by the superimposed Schumann resonance activity. Their results indicated the first Schumann resonance at approximately 8 Hz.

More recent work was accomplished in the low frequency ranges at the Naval Postgraduate School in Monterey, California. Barry (1978), Clayton (1979) and McDevitt and Homan (1980) investigated geomagnetic fluctuation in the frequency ranges .1-10 Hz, .4-40 Hz and .04-25 Hz, respectively. Their results are in general agreement with earlier measurements.

III. SYSTEM DESCRIPTION

A. REMOTE MONITORING SITE

The remote geomagnetic monitoring station was established primarily in support of the Naval Postgraduate School's research work on geomagnetic fluctuations on the ocean floor. To measure magnetic fluctuations on the sea floor, a source of reliable, nearby land reference data is needed. Precision time and frequency correlation of sea floor data with land data permits differentiation between the local sea-generated fields and those due to external sources. The remote monitoring site is located in the mountain 40 km. southeast of Monterey, California, in the Carmel Valley near the Tassajara Road entrance to the Los Padres National Forest (Figure 4). The hilltop altitude of 3844 feet with the additional 20 feet of antenna provides the needed elevation for VHF (138.7 and 140.2 MHz) propagation to the Naval Postgraduate School. This location is a magnetically quiet site, relatively close to the ocean (25 km.). The lack of low frequency industrial and power transmission interference coupled with an abundance of solar energy for power were also considered in the site selection. The basic telemetry design for the monitoring station was performed by Beliveau (1980).

At the base of the antenna, a storage cabinet was constructed to house the radio and electrical equipment. A solar array

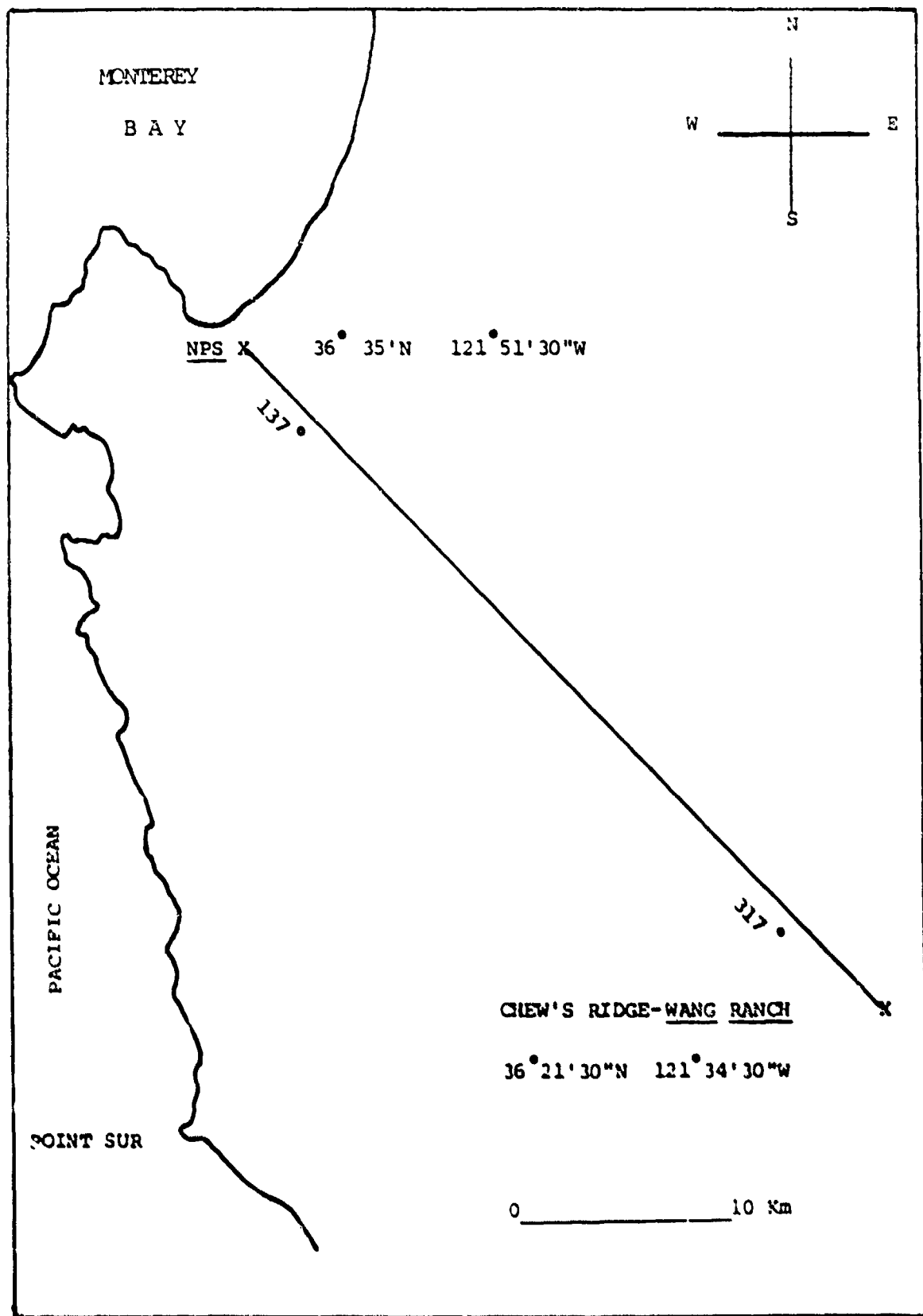


Figure 4. Chew's Ridge Site Location

was mounted on top of the cabinet and oriented for maximum power output. A single coil sensor was buried in a wooded area on the far side of the hillcrest, approximately 90 meters from the transmitter location.

B. SYSTEM COMPONENTS

The major parts of the system are shown in Figure 5, 6, and 7 and further details are given in Appendix A.

The sensor, a coil antenna, was oriented to measure fluctuations in the east-west component of the local magnetic field. As the field varies, small voltages are induced in the coil. These voltages are amplified and transmitted by cable to the storage cabinet where they are amplified a second time to the desired signal level. The resultant voltage variations are applied to a voltage controlled oscillator. As the magnetic field changes, it causes the VCO to vary about its free running frequency (1500 Hz). This time varying frequency is then transmitted by radio to an antenna atop Spanagel Hall at the Naval Postgraduate School.

The incoming signal is detected with a phase-lock loop that tracks the tone and removes any static bursts. The phase-lock loop frequency is recorded for later analysis.

During analysis the tape recorder output is demodulated with a frequency to voltage converter (FVC) producing a varying voltage directly proportional to the original output from the sensor coil. The VCO/FVC combination introduces a

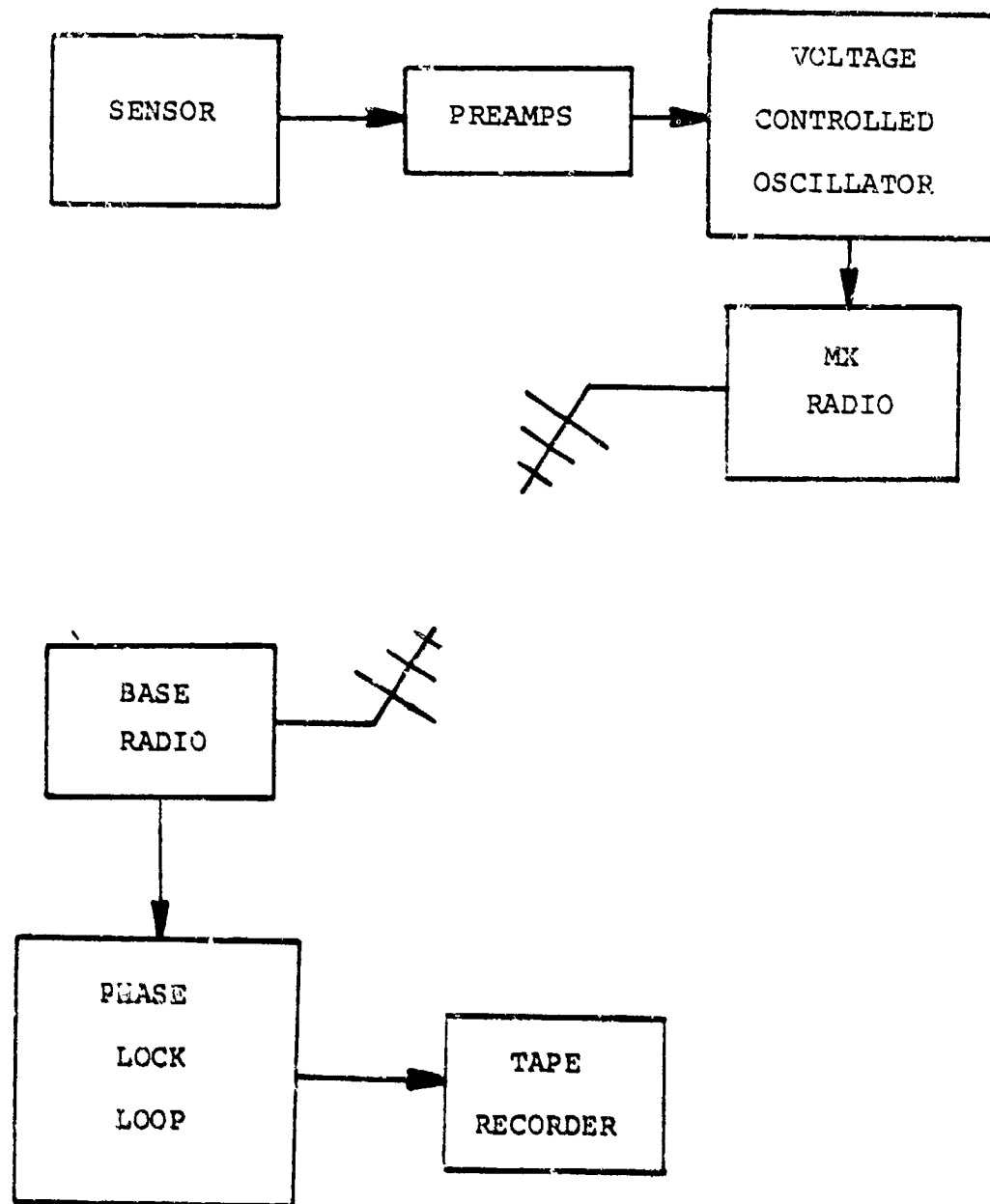


Figure 5. Data Collection System

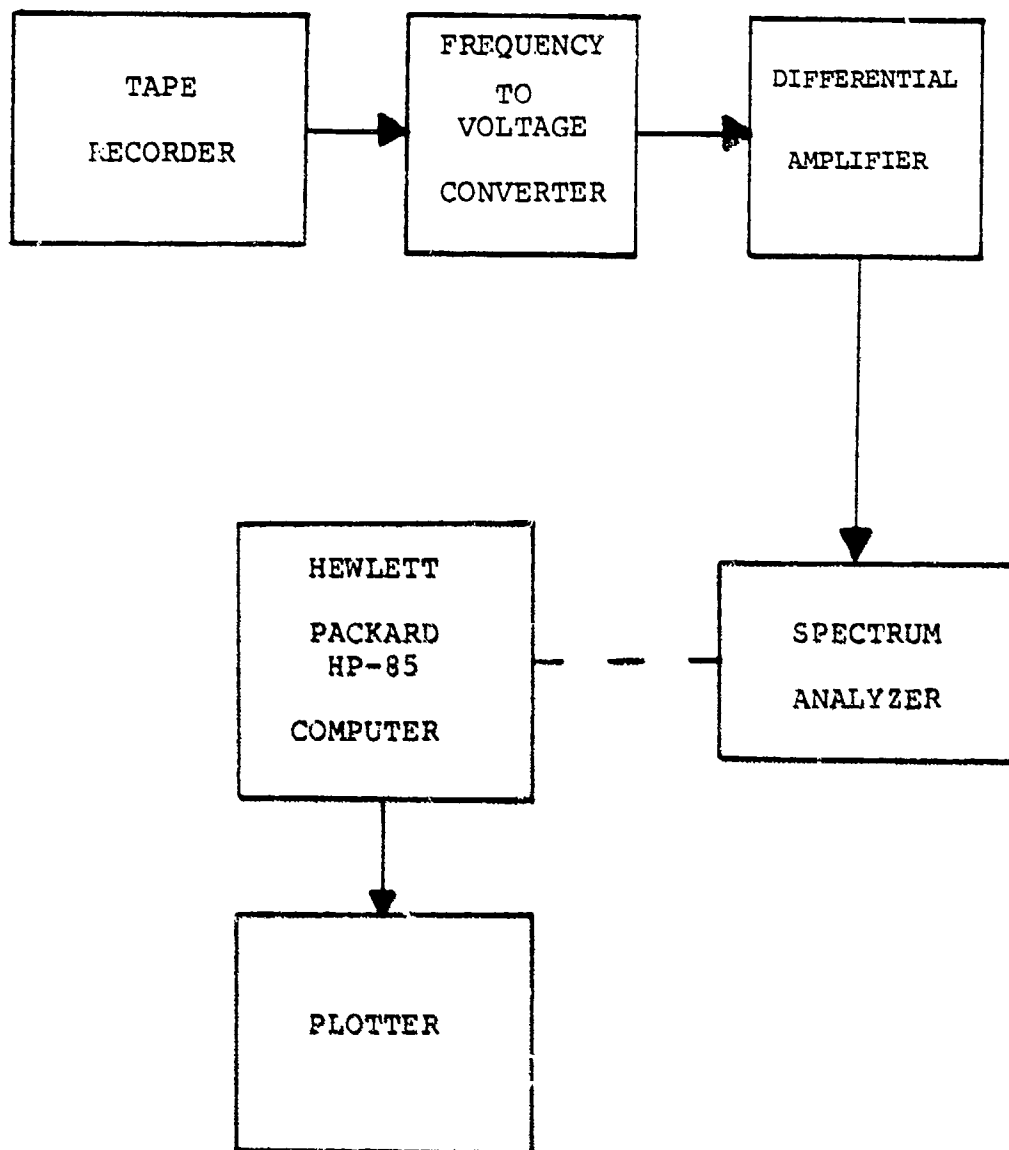


Figure 6. Data Processing Equipment

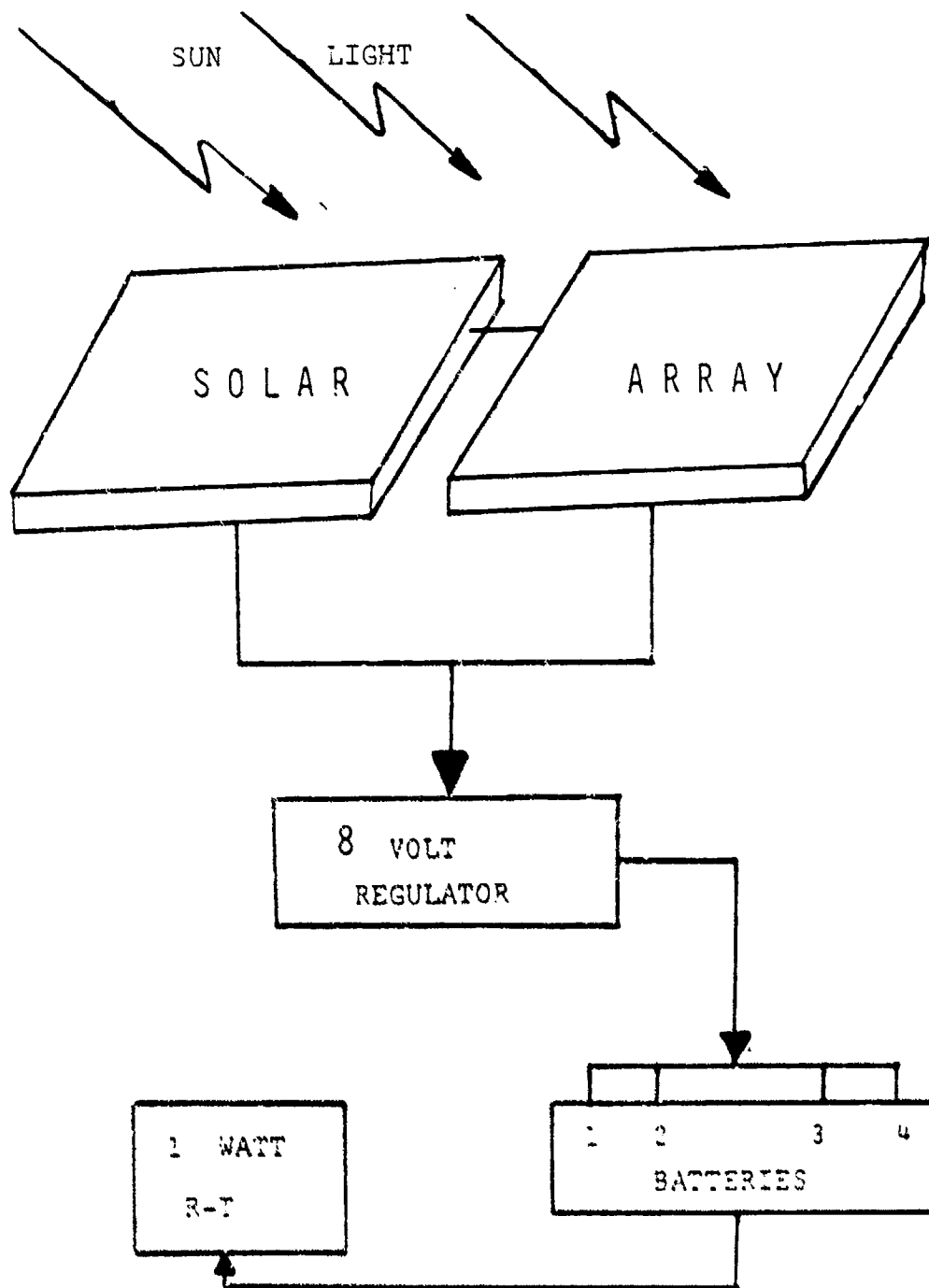


Figure 7. Radio Power Supply

a positive dc voltage offset that is removed with a differential amplifier. The resultant a.c. signal is processed by a spectrum analyzer that produces a 400 data point digital display. Data points thus obtained are entered into a Hewlett-Packard HP-85 computer. The HP-85 corrects each data point for the overall system gain function as well as for the spectrum analyzer bandwidth. (Section III, C and D). The final processed data is plotted with a Hewlett-Packard 7225A plotter. A more detailed discussion of the pieces of equipment and their characteristics is contained in Appendix A.

C. SYSTEM TRANSFER FUNCTION

The entire system can be represented by a block diagram that converts a fluctuating magnetic field into a voltage that can be displayed and whose power spectral density can be measured with a spectrum analyzer.



Since the transfer function, $H(f)$, is frequency dependent, it was calculated by dividing the system into components as shown below. The sensitivity of each component was found over the frequency range of interest and then added point by point to produce the system transfer function.

The radio, phase-lock loop, tape recorder and differential amplifier are all of unity gain and do not affect the transfer function calculation. The data presented in this research is

SYSTEM TRANSFER FUNCTION

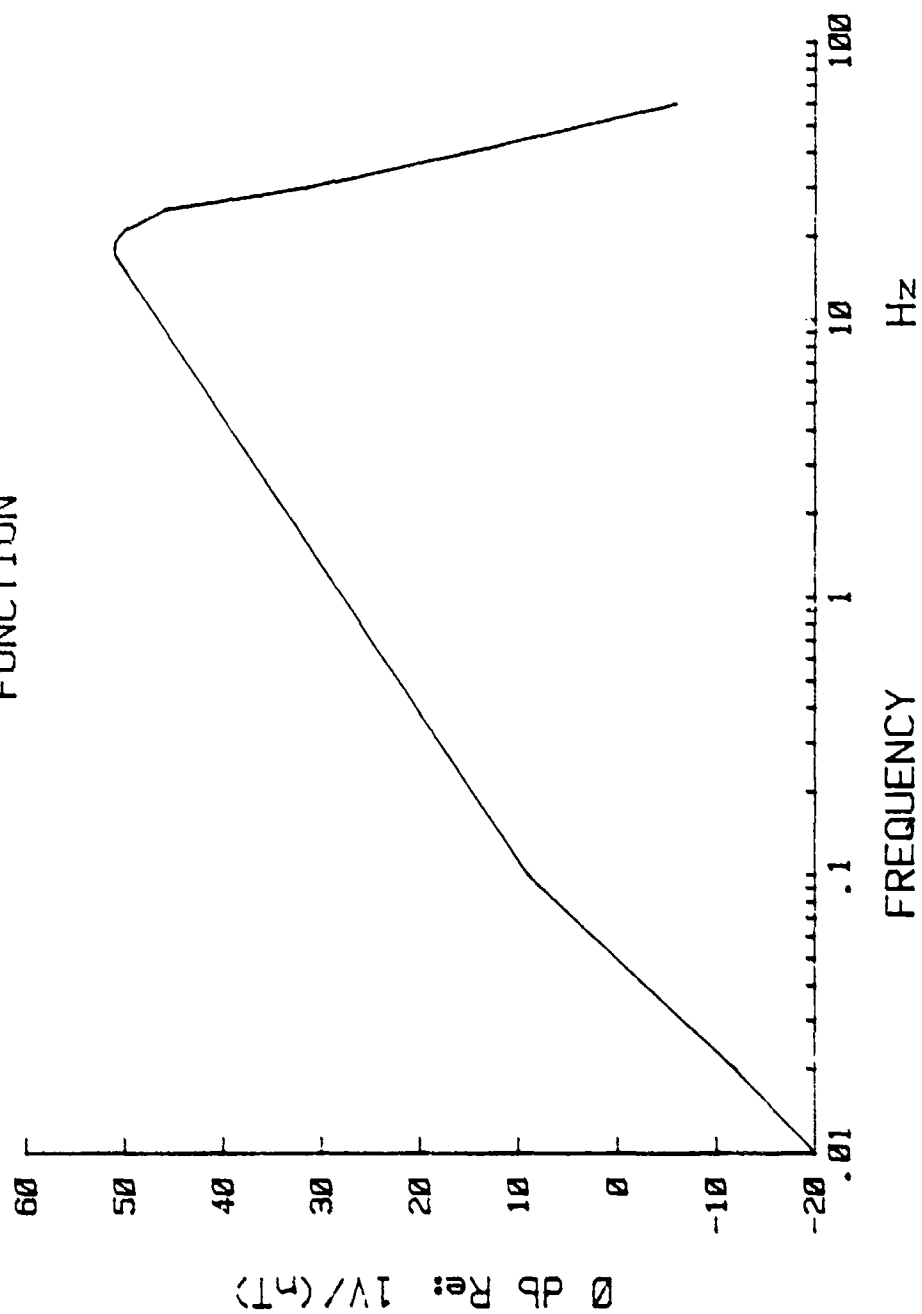
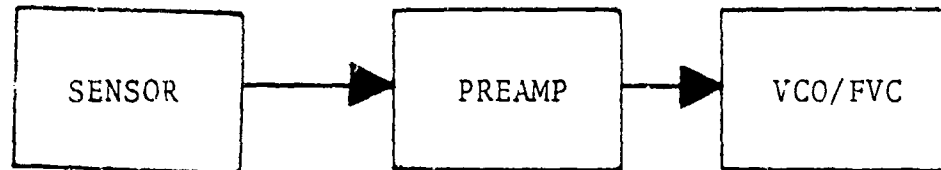


Figure 8. System Transfer Function

referenced to 1 nT in order to be consistent with earlier work. Details of the procedure used are described in Appendix B, Sections I and II.



Given the system transfer function, the corrected power spectral density can be found from

$$P = N - 10 \log |H(f)|^2$$

where

N = The Spectrum Analyzer reading in db, referenced to 1 volt

HW = The Hanning window bandwidth correction for the particular Spectrum Analyzer used in db

$H(f)$ = The transfer function defined above

P = The corrected power spectral density where 0 db is referenced to 1 nT²/Hz

D. SYSTEM NOISE

The major source of the total system noise is that introduced by the preamplifier located at the sensor. The best amplifier performance is achieved when the amplifier causes the least decrease in the overall signal-to-noise ratio. The preamplifier in this system, Model 13-10A, was selected because it possesses a better signal-to-noise ratio and improved low noise characteristics when compared with Model 13-10 which was used in the earlier work of McDevitt and Homan, (1980).

To compare the two preamplifiers, a 120 Ω resistor was connected across the input while the rms output voltage was measured in the spectrum analyzer. Figure 9 shows that approximately 10 dB of improvement was obtained at .1 Hz by using the Model 13-10A.

The total system noise rms voltage level was measured several times. A 120 Ω resistor (to replace the 124 Ω sensor coil) was connected to the preamplifier input and normal analysis of the resulting transmitted signal was performed. The resulting system noise obtained is shown in Figure 10. A comparison with the noise measured by McDevitt and Homan at Chew's Ridge shows that the telemetry system noise was 15 dB \pm 5 db lower over the frequency range of 1-20 Hz. As discussed above the main reason for this difference is the use of the improved preamplifier. The remaining improvement, reduction in system noise, is due mainly to the substitution of an instrumentation tape recorder for the portable stereo cassette type used by McDevitt and Homan.

PREAMPLIFIER (120 OHM RESISTOR) NOISE VS FREQUENCY

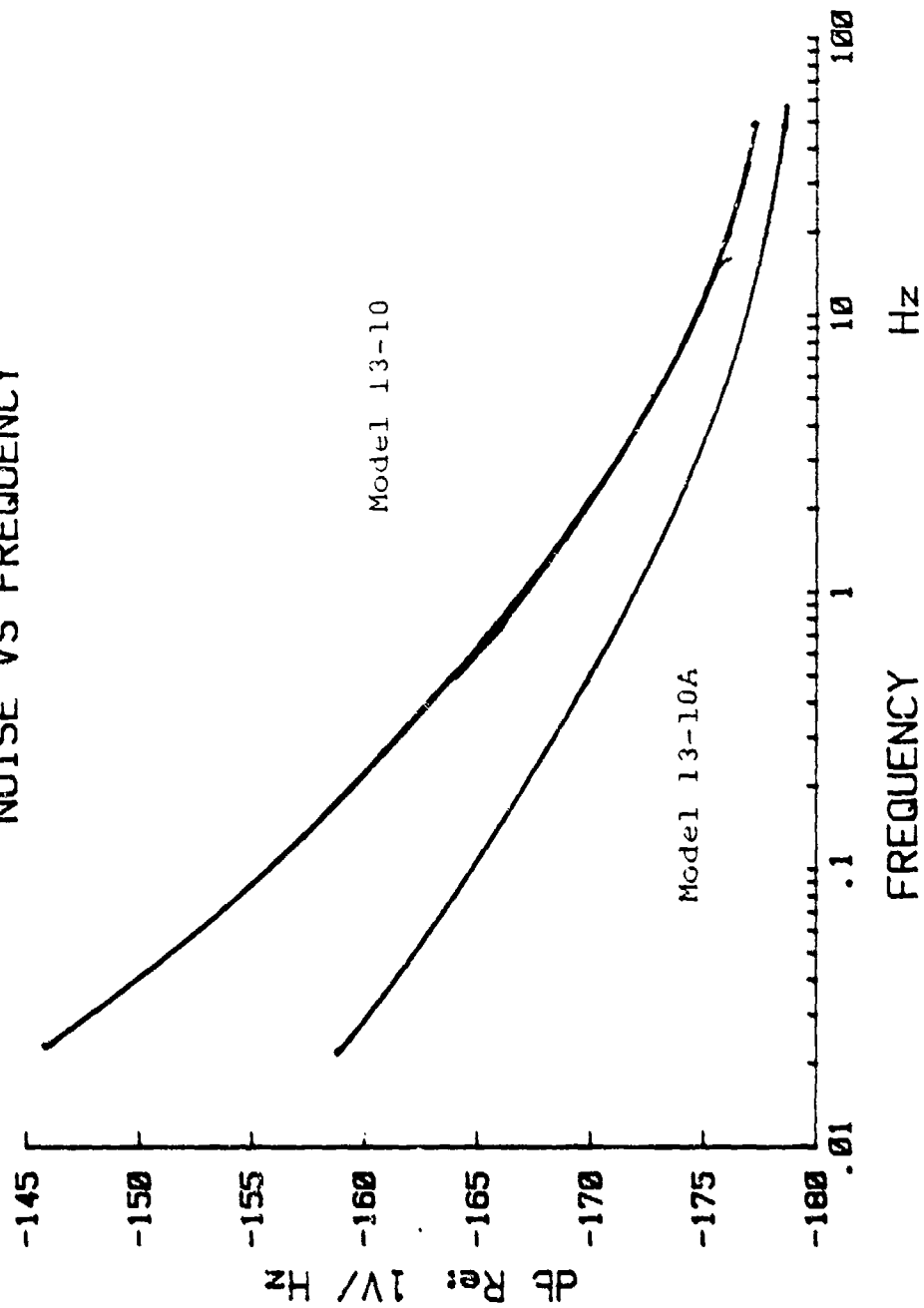


Figure 9. Preamplifier Noise Comparison

CHEW'S RIDGE EAST-WEST COMPONENT

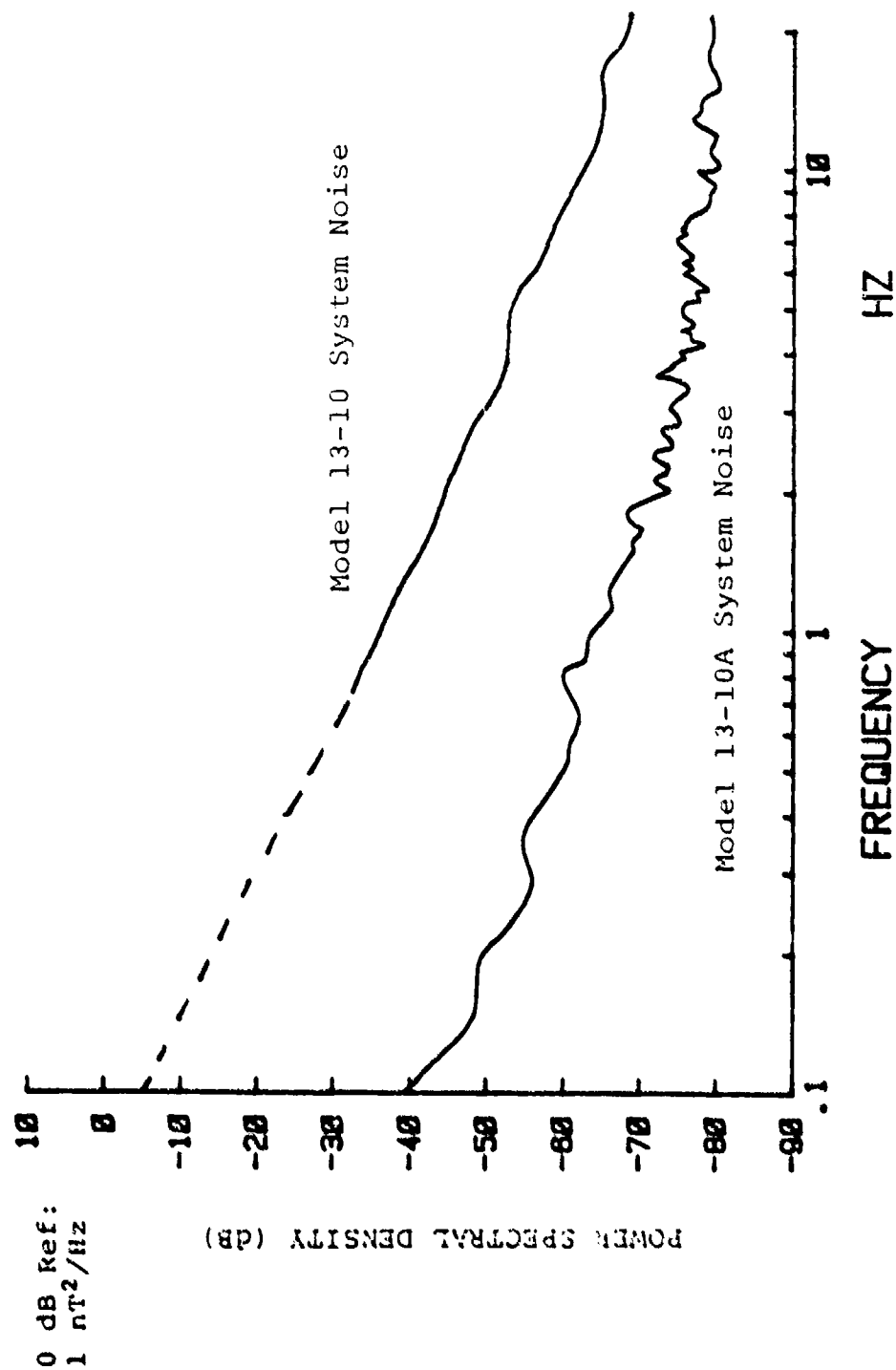


Figure 10. System Noise

IV. EXPERIMENTAL RESULTS

A. INTRODUCTION

During the months of July, August, September, and October, 1981, a total of 68 hours of data was collected. Four specific time intervals, 0730-0900, 1100-1230, 1800-1930 and 2300-0030 were selected each day. Approximately the first 45 hours of data were subject to static bursts in the telemetry transmission that prevented analysis by long (N greater than 8) time averages of the data. During this initial installation phase, numerous equipment adjustments and modifications were made. The data presented represent measurements obtained from the final system (4-5 October, 1980) and data taken concurrently with undersea measurements made by (Ames and Vehlsage, 1981) on 21 and 24-25 August, 1981.

Comparisons were made of the power spectral density for each of the above time frames for a number of days. Comparisons were also made for spectra at different times of the day to determine daily variations. The data was correlated with previous data to show compatability for each time period using quiet days selected from the data. The days of varying degrees of magnetic activity were investigated separately.

The level of magnetic activity was determined by using the daily 24-hour A-index and the 3-hour K-indices measured

at the Fredericksburg, Virginia (mid-latitude) magnetic monitoring station. The Space Environment Services Center located in Boulder, Colorado, publishes a Preliminary Report and Forecast of Solar Geophysical Data, including geomagnetic activity. A more detailed synopsis of geophysical data is contained in the environmental data services monthly publication "Solar-Geophysical Data". The A-indices range from 0 (very quiet) to 400 (extremely disturbed) with an A-index of 30 or greater, indicating geomagnetic storm conditions. The K-indices range from 0 (very quiet) to 9 (extremely disturbed).

The position of the Chew's Ridge sensor was fixed, to measure the East-West component of the local magnetic field, as shown in Figure 11.

B. REVIEW OF DATA

Figures 12-27 represent eight separate data tapes. Each data tape was analyzed over two frequency scales, .01-5 Hz and .1-20 Hz. Due to differing amounts of time required to produce each average, a larger portion of the tape was analyzed for the .01-5 Hz average. In an effort to minimize differences between the two scales, the .1-20 Hz average was made from the approximate center of the tape used for the .01-5 Hz average. Figure 28 is an average of all daytime and nighttime data recorded during the project.

The data presented in Figures 12-19 represent four measurements taken concurrently with undersea measurements

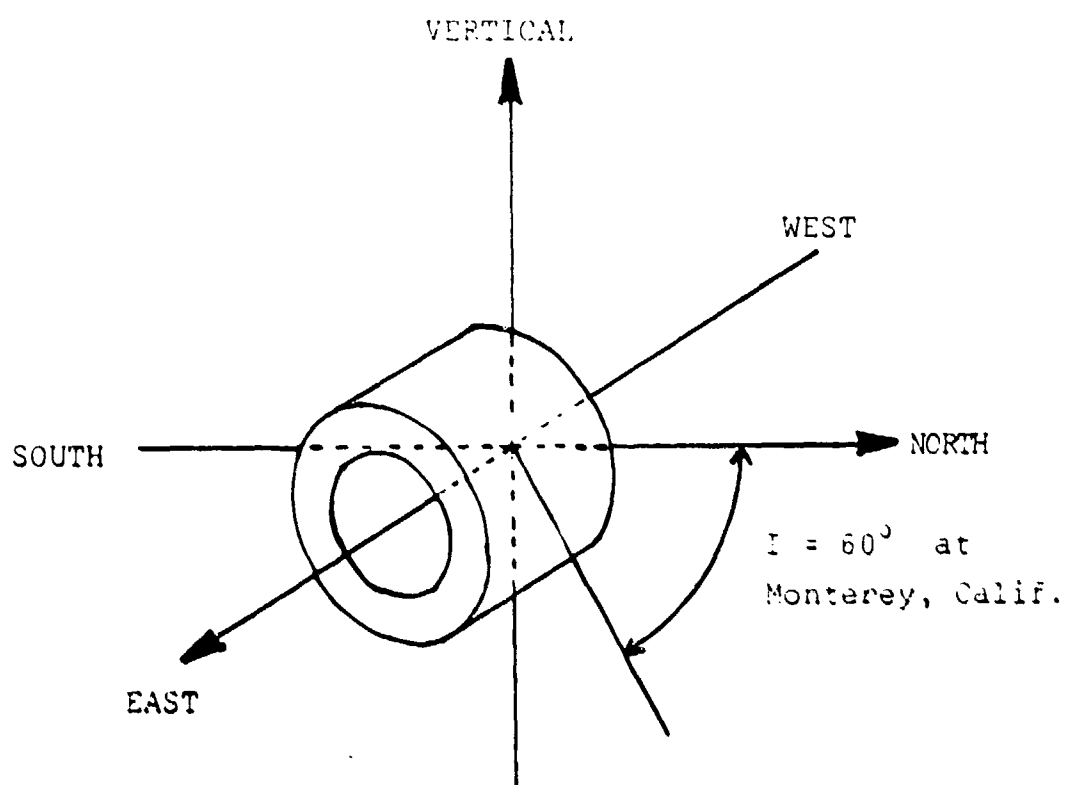


Figure 11. Chew's Ridge Sensor Orientation

made by (Ames and Vehlsage) on 21 and 24-25 August from the Research Vessel Acania. The nature of the underwater data collection system made it necessary to deviate from the normal collection schedule. The underwater system, when placed on the sea floor, used a timer to start its recorder after the ship had moved far enough away to no longer affect the readings. Once a thirty-minute tape had been recorded, the system had to be recovered, reset and once again lowered to the ocean floor. The normal two hour turnaround time for this operation was subject to numerous possible delays. In order to make the concurrent measurements, the Research Vessel Acania, radioed each start time to the Chew's Ridge recording site in Spanagel Hall at the Naval Postgraduate School. The land recordings were started within ± 30 seconds of the sea recordings, in all cases.

The August measurements were made prior to the addition of a 14 dB amplifier that was included in the final system; therefore, the transfer function used in processing this data was 14 db lower than the one given in Section III. The power spectral density for each E-W Chew's Ridge measurement was compared to the results of the horizontal component measurement obtained from the undersea measurement.

Three of the four land-sea measurements were in excellent agreement. Figures 13, 17 and 19 (the midday, night and sunrise spectra for the .1-20 Hz scale) are consistently 3-7 db higher than those measured underwater. In addition

individual peaks observed exhibit a 90% correlation. A difference in relative magnitude between the peak in the two sets of data was noted. This is probably due to the fact that the land data was fixed to measure the East-West component, while the sea data system measured a horizontal component of unknown orientation.

The fourth land-sea comparison, Figures 14 and 15, is interesting in two aspects. First, the power spectral density on the .1-20 Hz scale (Figure 15) for the local sunset, 1935 hours on 24 August, is the lowest of the day. On the .01-5 Hz scale however, the measurement crosses over the other measurements for the day for frequencies less than .1 Hz and reaches the highest level measured to date on the system. Secondly, the fact that this measurement occurred on a day with an A index of 15 and K's of 3's made this spectrum suspect. The concurrent underwater measurements also showed an even greater surge of power spectral density increase across the entire frequency scale that was 30 dB greater than that recorded on the land system. The correlation between the individual peaks of the two sets of spectra was very poor and makes this result questionable. Another indication that this time period was nontypical is that the local night measurement, Figures 16 and 17, were among the highest recorded for the entire day, a result just opposite of what was normally observed.

21 AUG 1345 HRS

CHEW'S RIDGE EAST-WEST COMPONENT

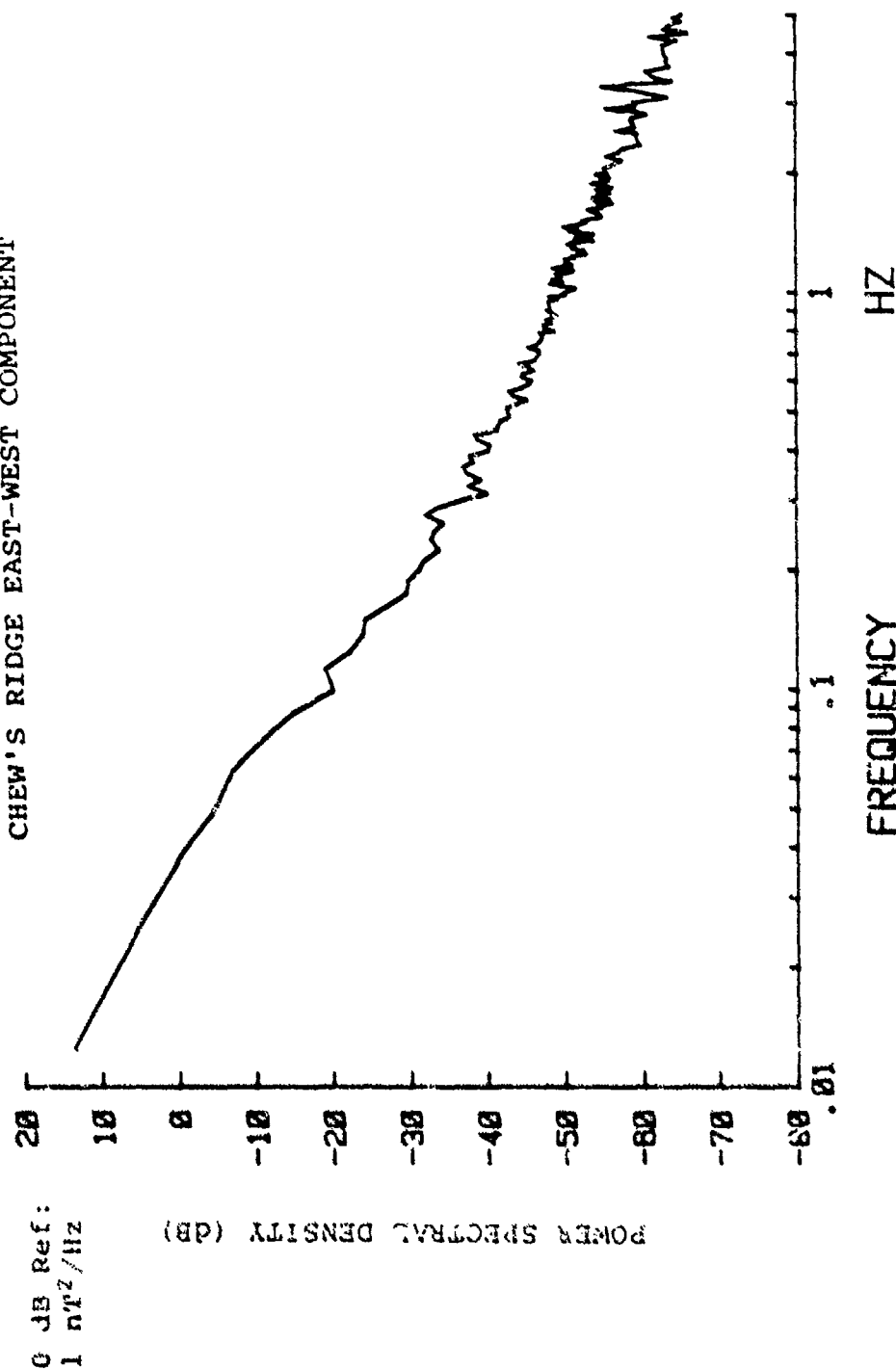


Figure 12. East-West Magnetic Field Fluctuations (.01-5 Hz)

21 AUG 1345 HRS

CHEW'S RIDGE EAST-WEST COMPONENT

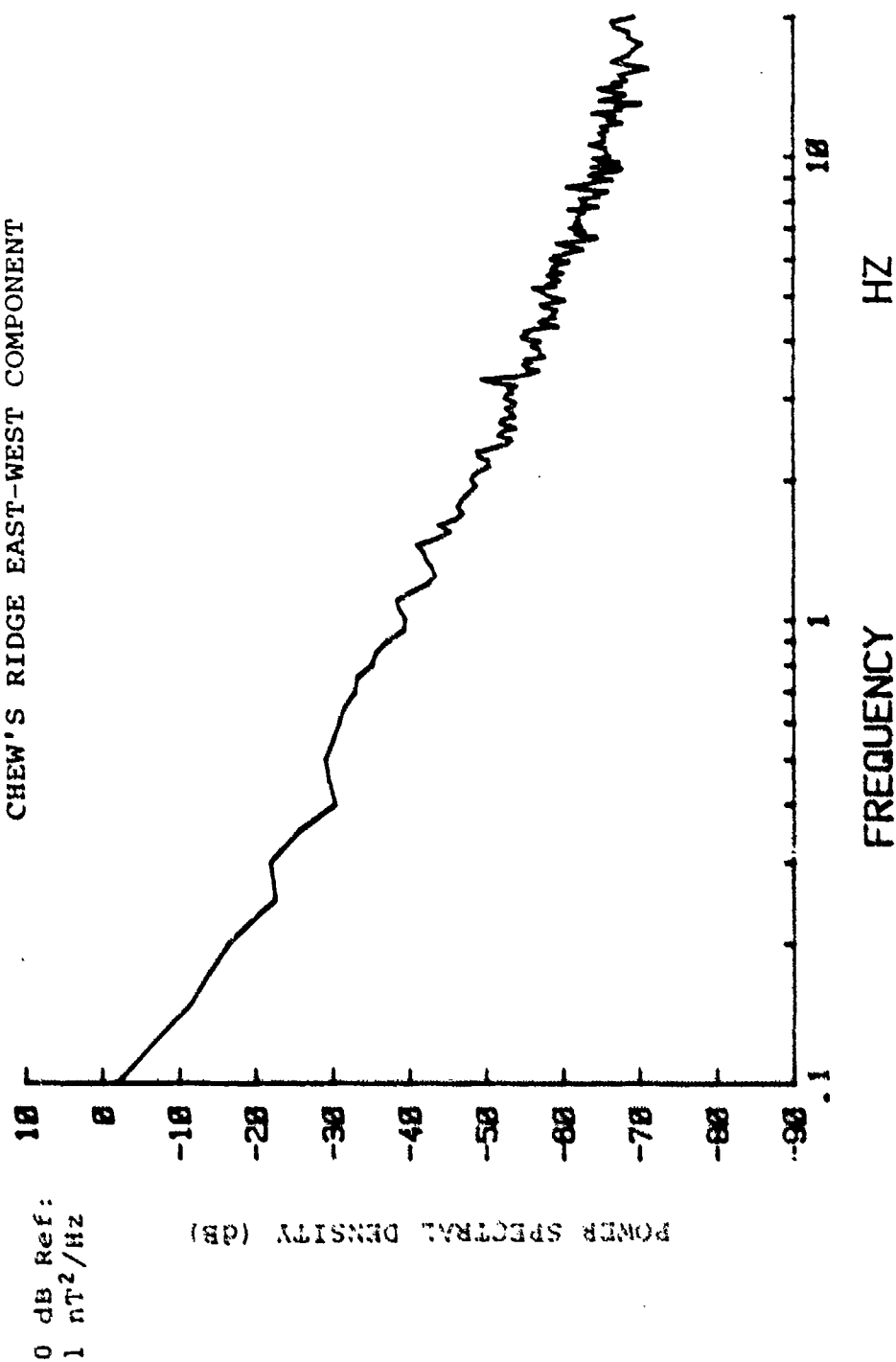


Figure 13. East-West Magnetic Field Fluctuations (.1-20 Hz)

24 AUG 1935 HRS

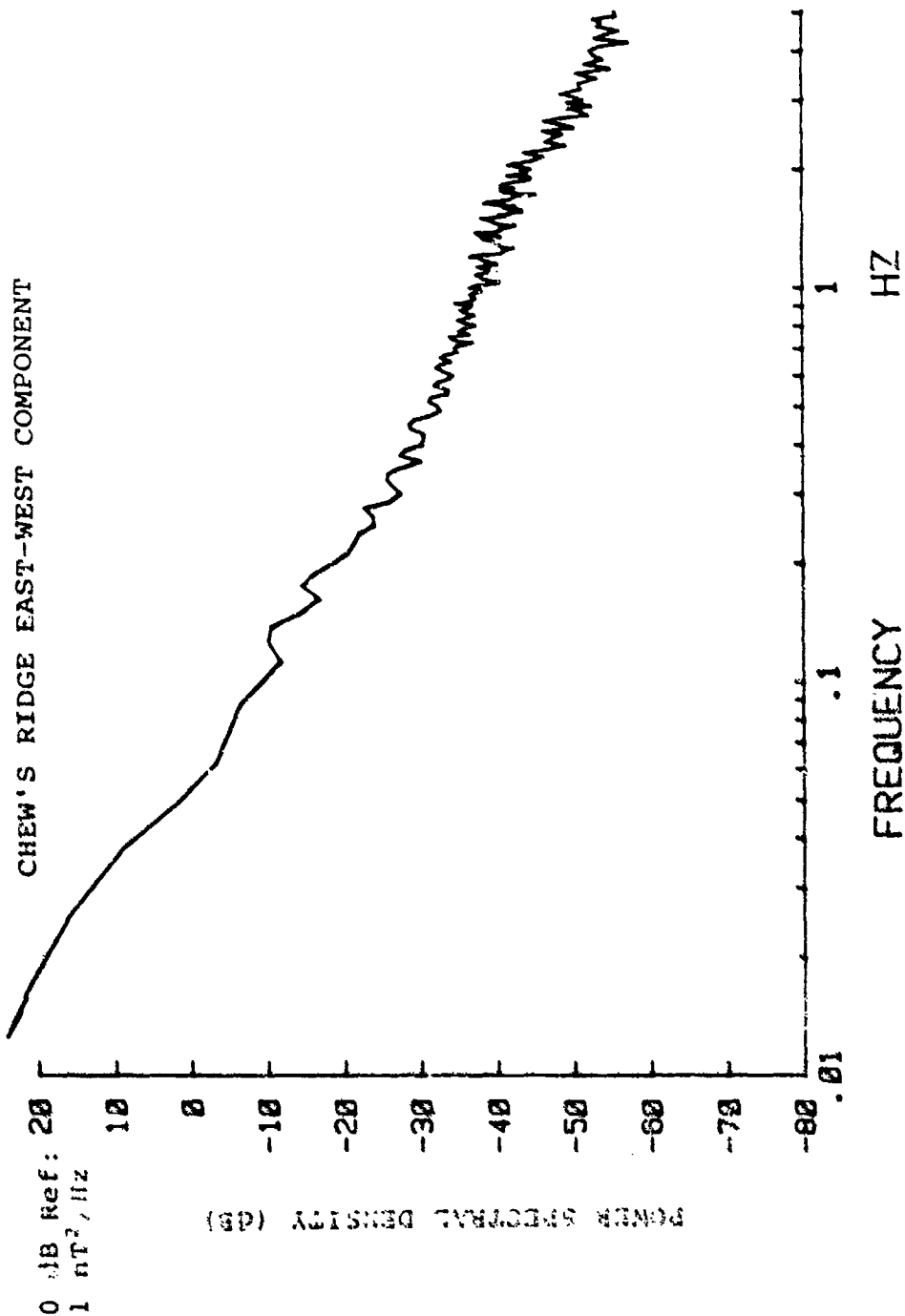


Figure 14. East-West Magnetic Field Fluctuations (.01-5 Hz)

24 AUG 1935 HRS

CHEW'S RIDGE EAST-WEST COMPONENT

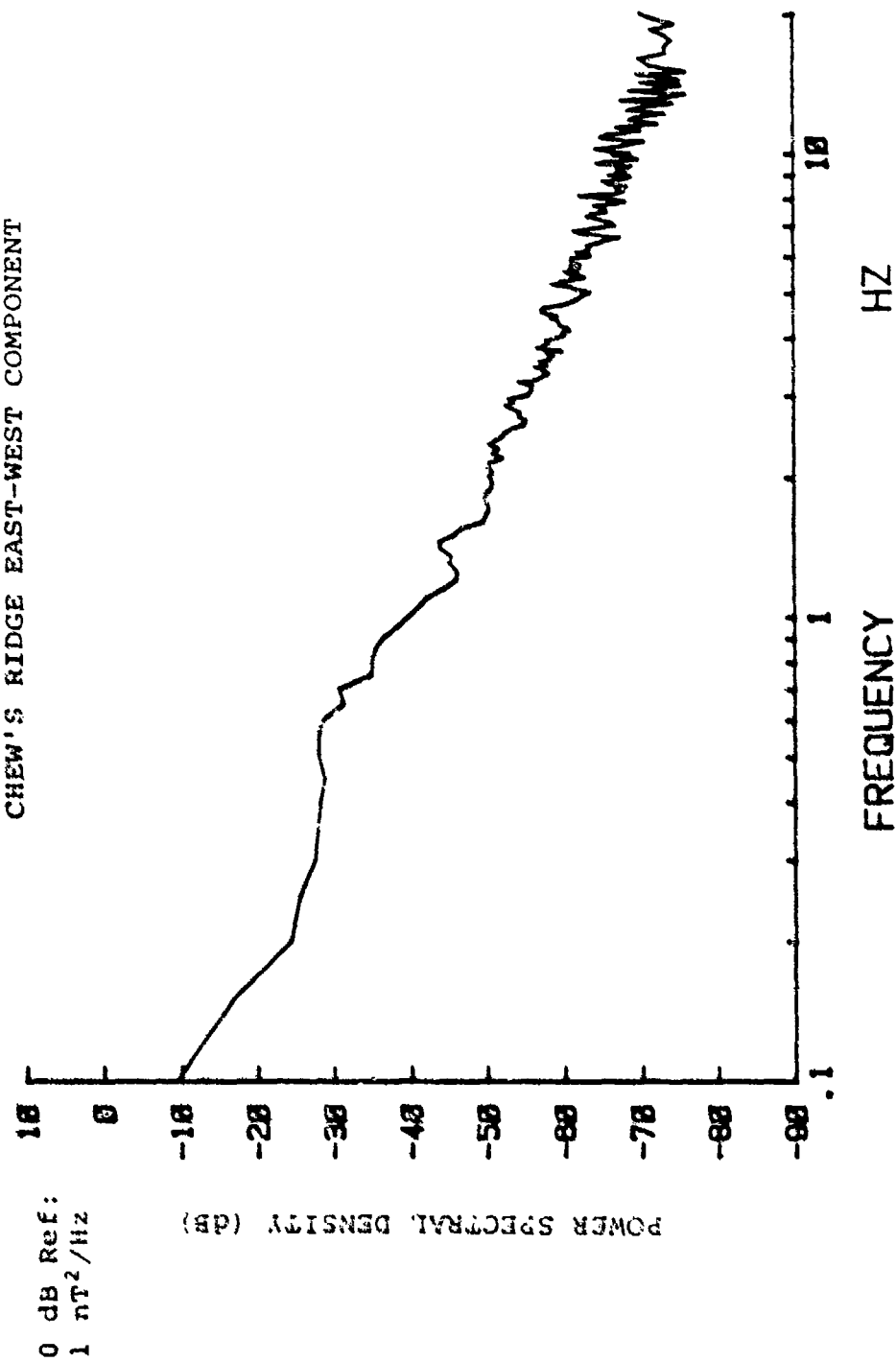


Figure 15. East-West Magnetic Field Fluctuations (.1-20 Hz)

25 AUG 0045 HRS

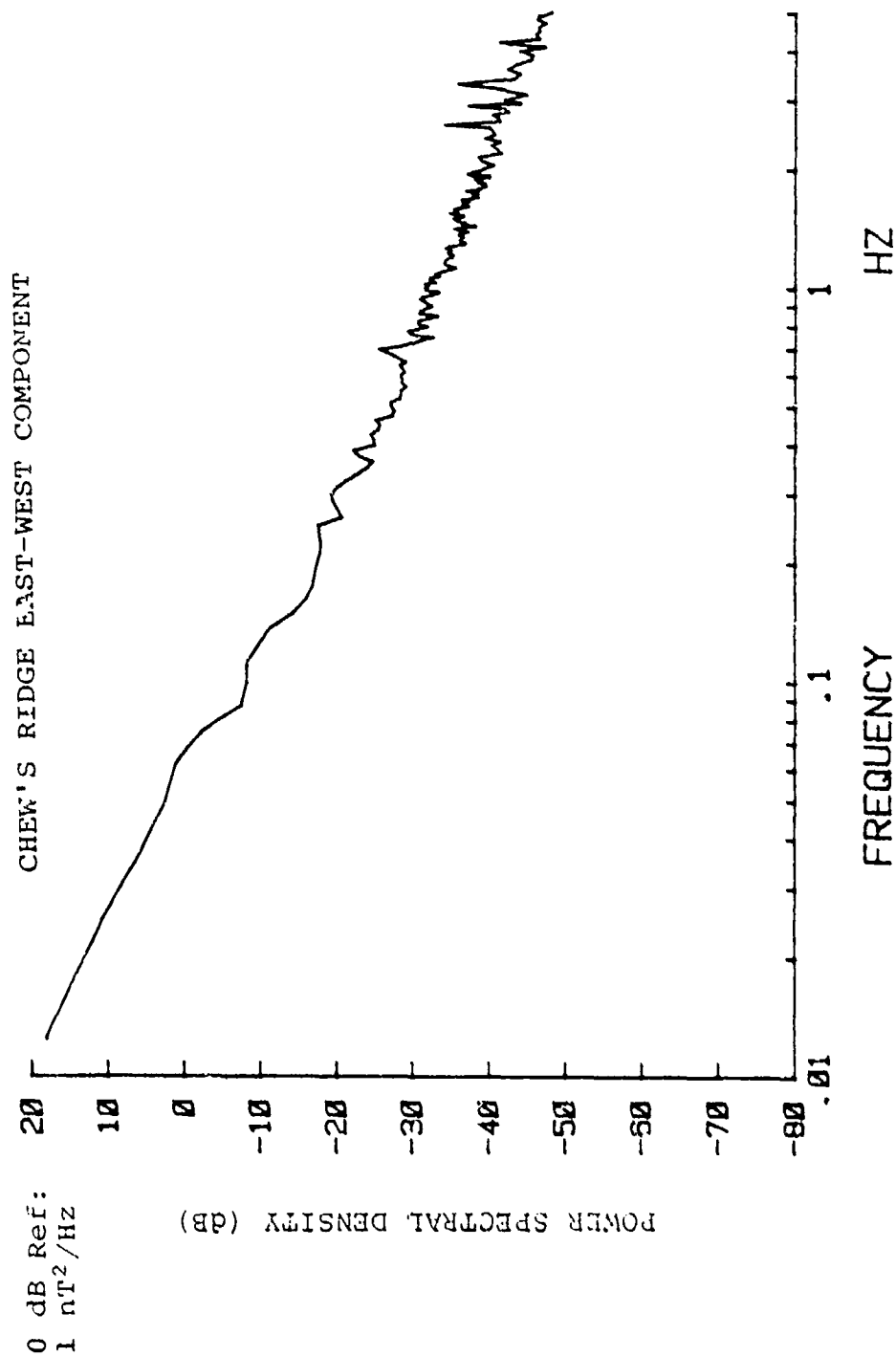


Figure 16. East-West Magnetic Field Fluctuations (.01-5 Hz)

25 AUG 0045 HRS

CHEW'S RIDGE EAST-WEST COMPONENT

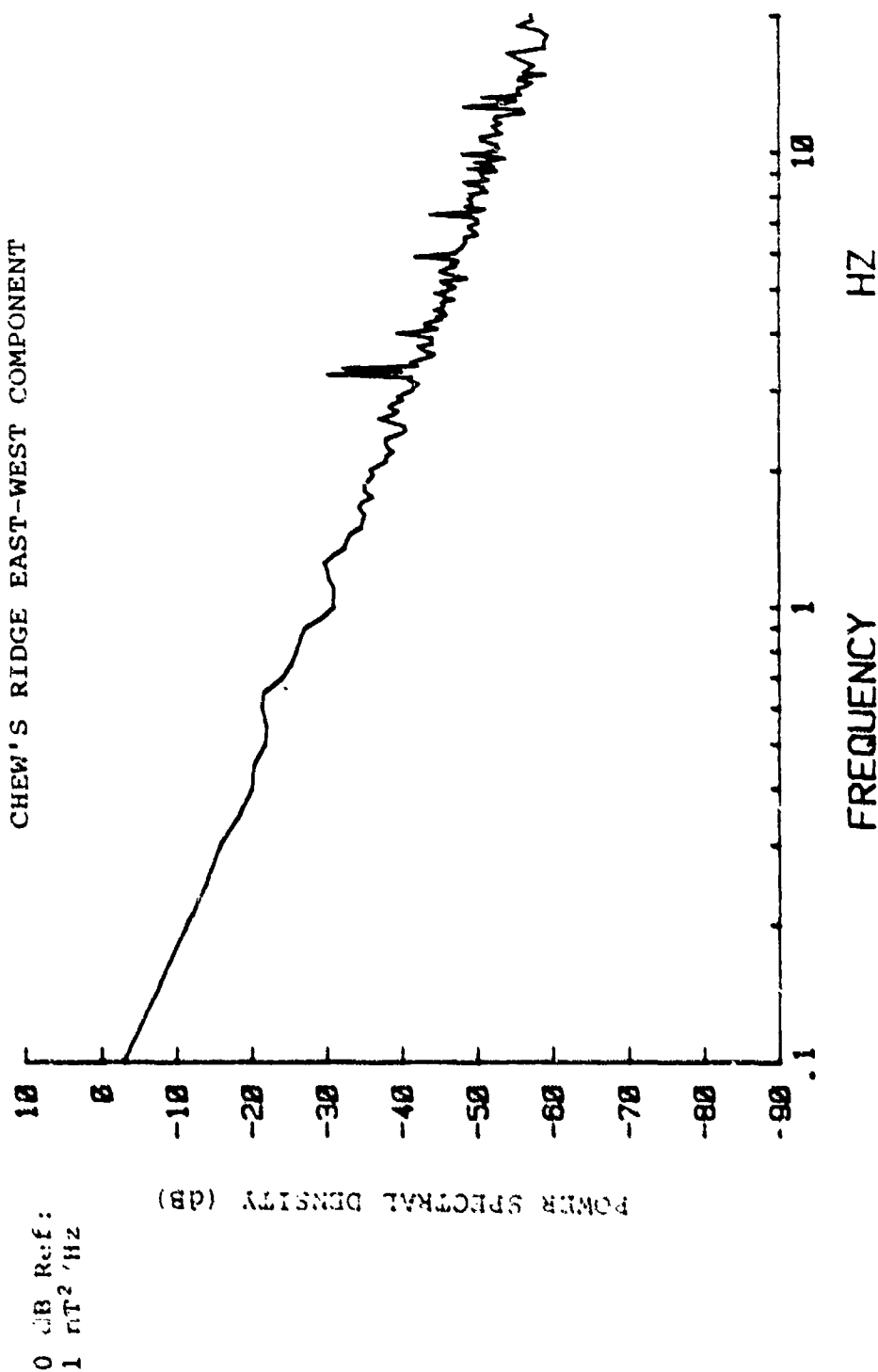


Figure 17. East-West Magnetic Field Fluctuations (.1-20 Hz)

25 AUG 0618 HRS

CHEW'S RIDGE EAST-WEST COMPONENT

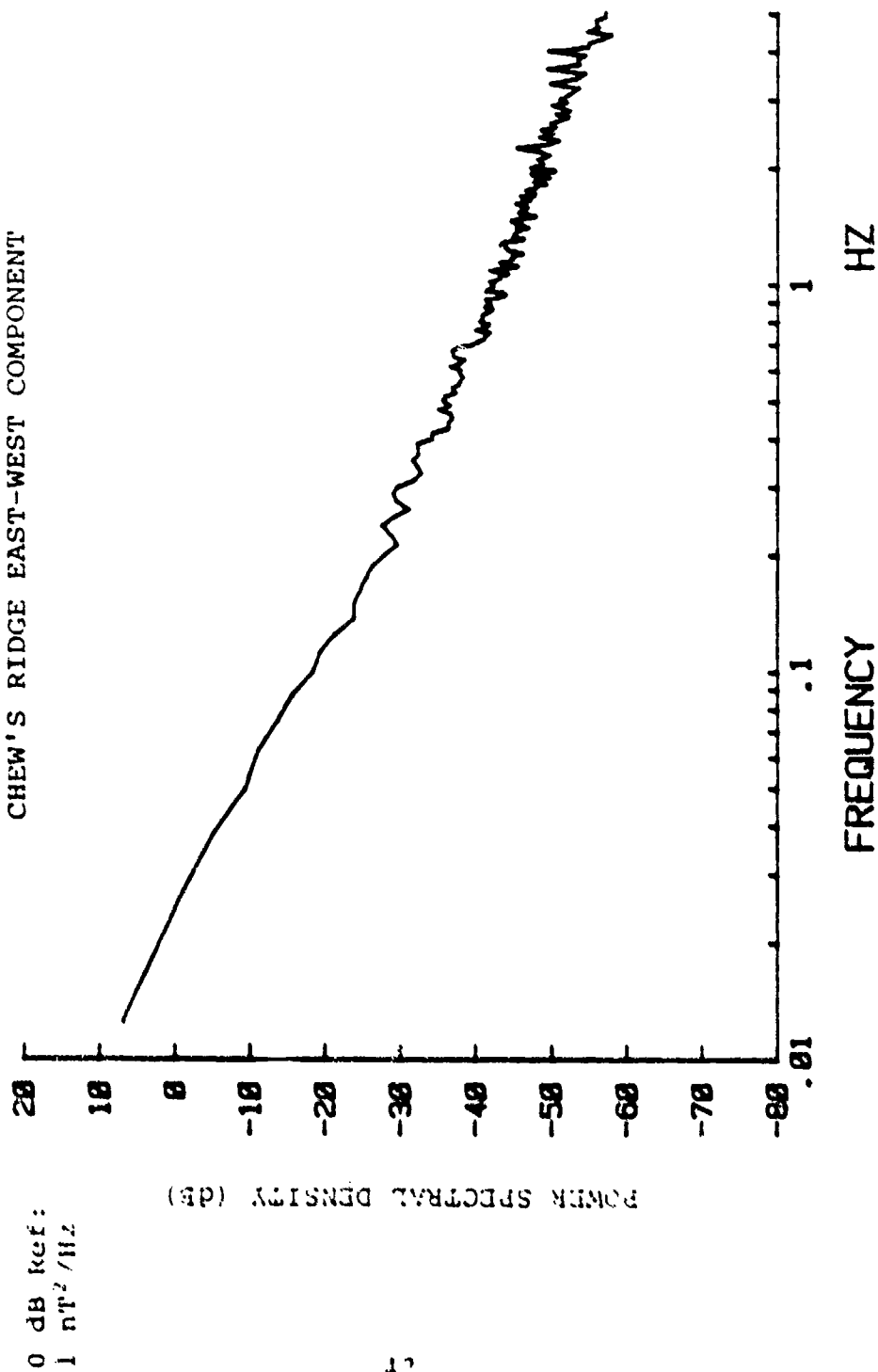


Figure 18. East-West Magnetic Field Fluctuations (.01-5 Hz)

25 AUG 0618 HRS

CHEW'S RIDGE EAST-WEST COMPONENT

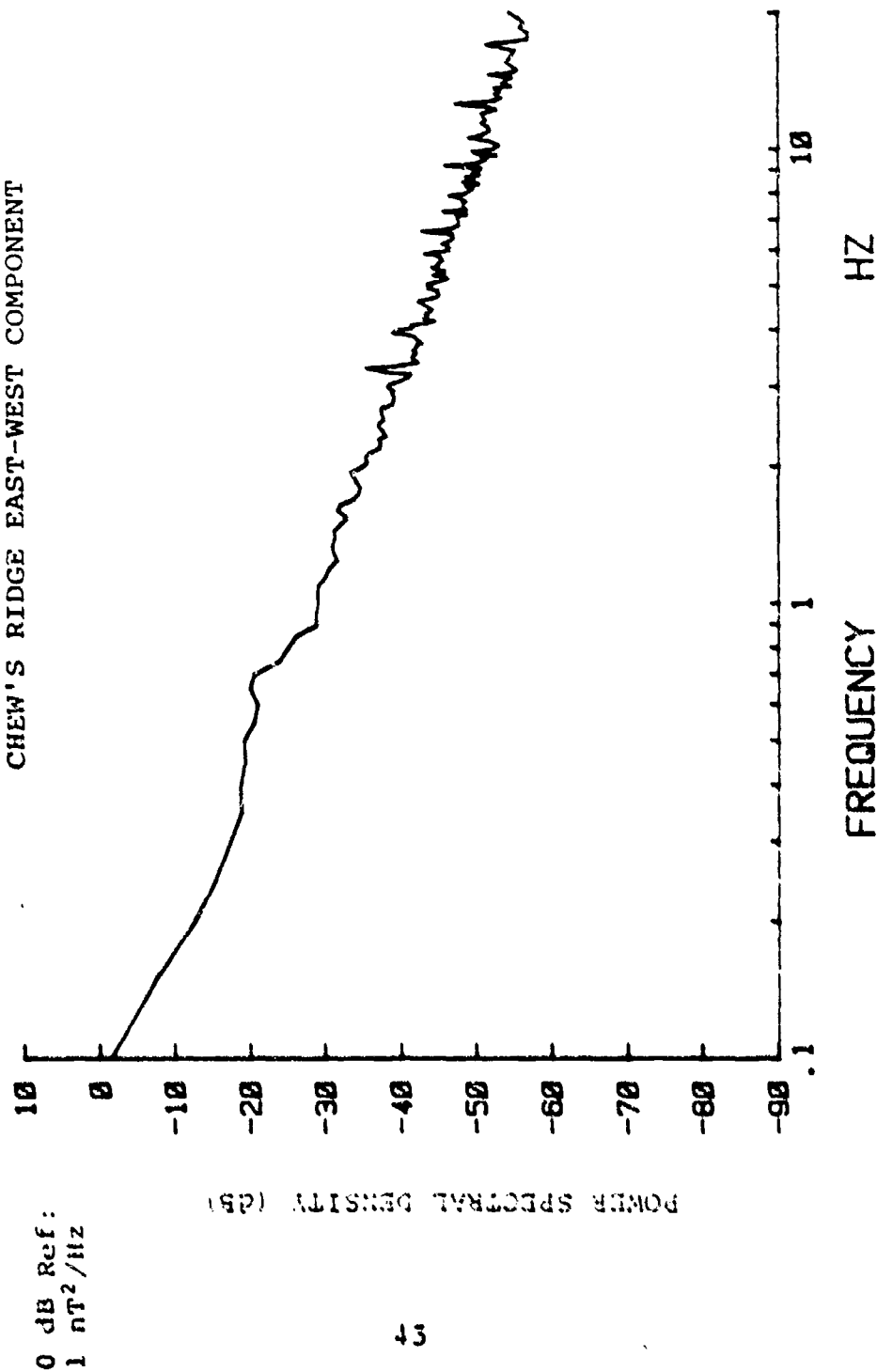


Figure 19. East-West Magnetic Field Fluctuations (.1-20 Hz)

The spectra in Figures 20-27 were obtained from data taken during normal recording operations on 4-5 October, 1981. The geomagnetic activity level was active to near storm levels, A = 24, and K's were mostly 4's and 5's, during this period. This set of spectra is characterized by more prominent peaks (up to 10 dB) than was observed in the August data. A sharp peak is seen at approximately 1.8 Hz in both the .1-20 Hz and .01-5 Hz graphs for 0830 hours on 5 October (Figures 26 and 27). This appears to be a large scale Pc1 event associated with the magnetic storm activity. It is also near the typical 2 Hz peak seen in the average nighttime data (Figure 28). A second interesting feature in this set of spectra is the splitting, or apparent splitting, of the 8 Hz Schumann resonance peak into a doublet with one subsidiary peak near 8 Hz and the other near 10 Hz in Figure 25 (4 October, 2330 Hours). While this phenomenon was not as obvious as that noted by Fraser-Smith (1975) in his North-South component research, it does seem to occur approximately 10% of the time and to remain for several hours during each occurrence.

Figure 28 shows the average East-West component during local day and night measurements for the period August-October, 1981. (Local California time listed on the graphs was 7 hours behind UT during this time frame.) On the average there was a noticeable decline in the geomagnetic activity level at night. The decline is most often seen at the low frequencies:

4 OCT 1130 HRS

CHEW'S RIDGE EAST-WEST COMPONENT

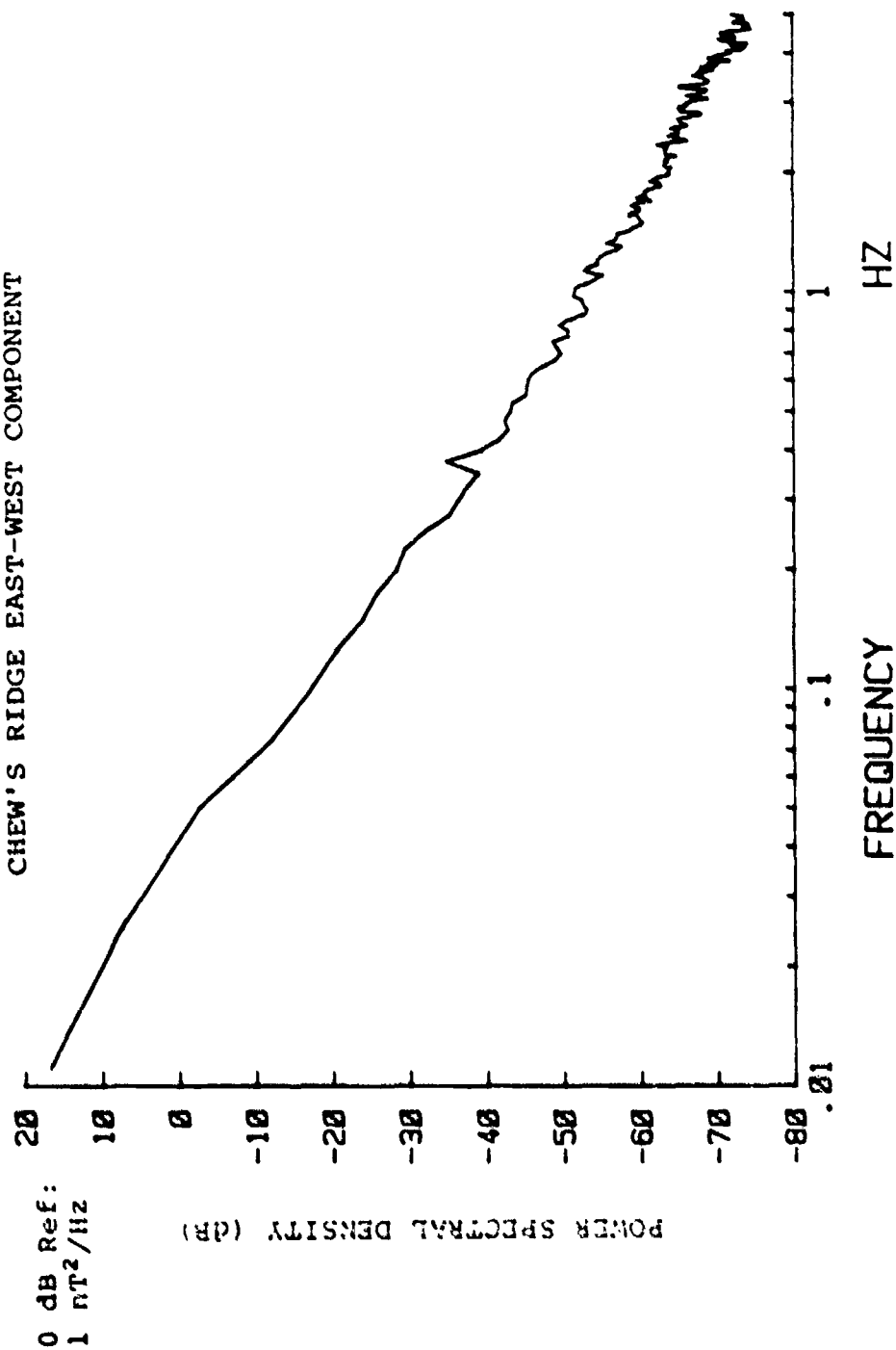


Figure 20. East-West Magnetic Field Fluctuations (.01-5 Hz)

4 OCT 1125 HRS

CHEW'S RIDGE EAST-WEST COMPONENT

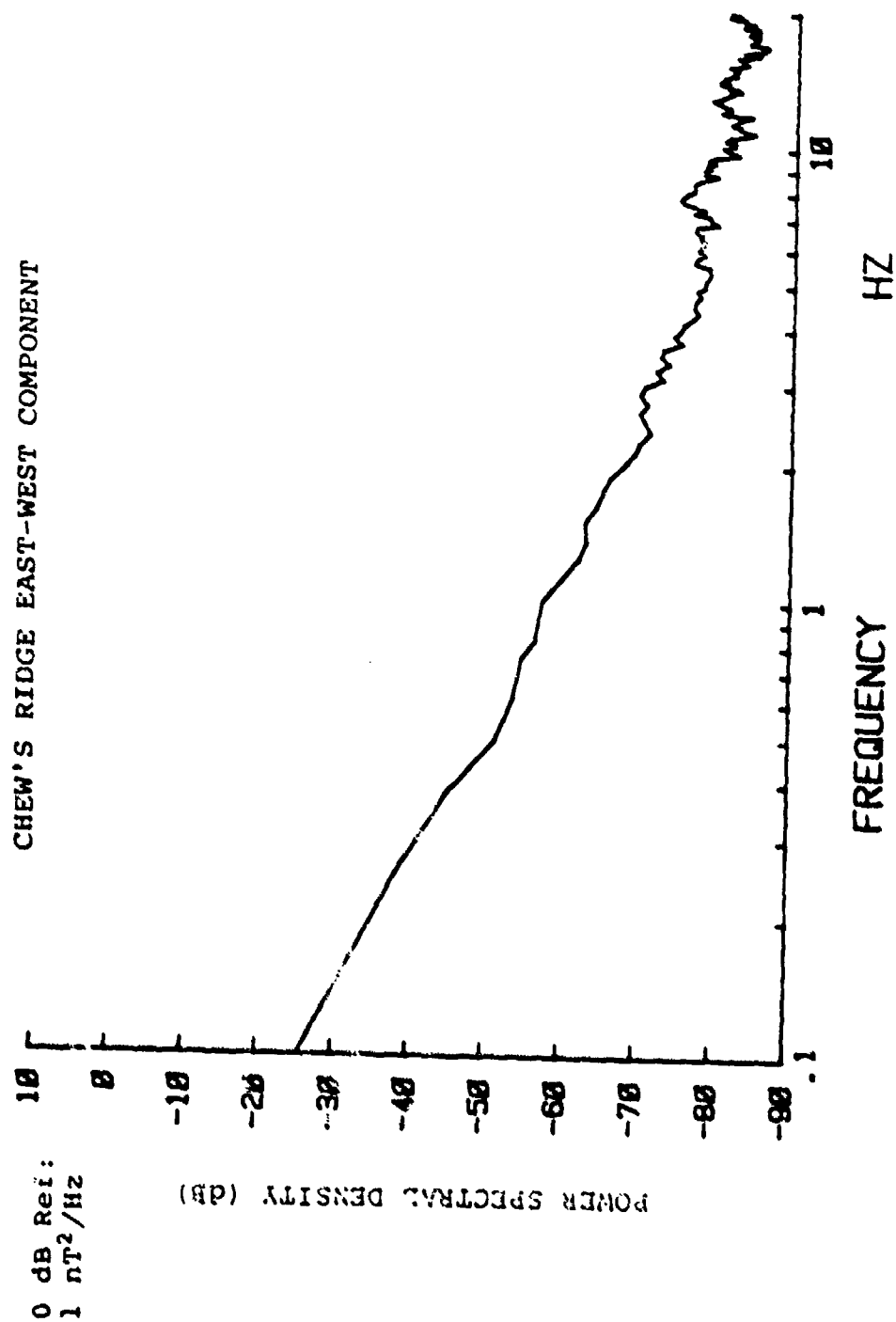


Figure 21. East-West Magnetic Field Fluctuations (.1-20 Hz)

4 OCT 1855 HRS

CHEW'S RIDGE EAST-WEST COMPONENT

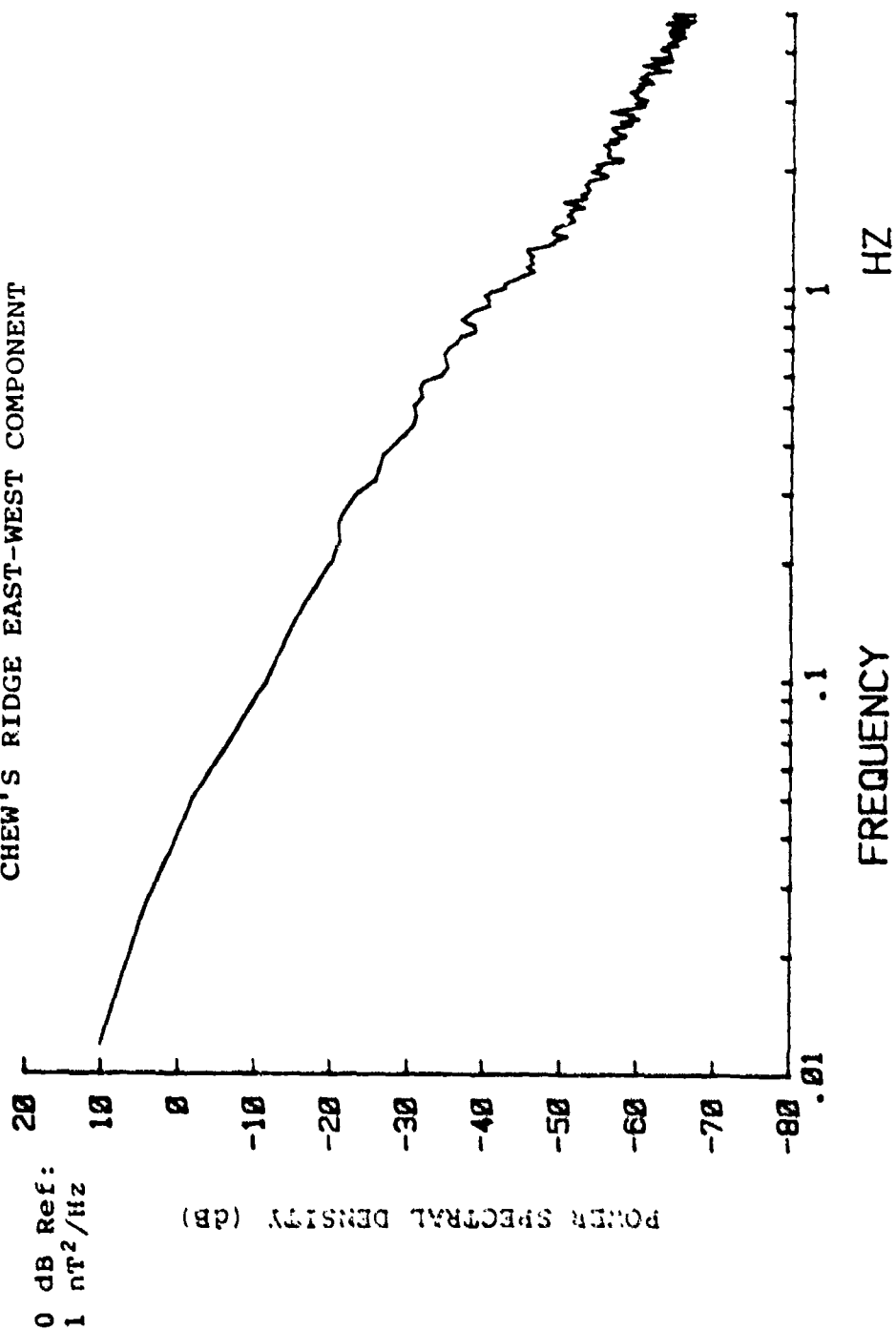


Figure 22. East-West Magnetic Field Fluctuations (.01-5 Hz)

4 OCT 1855 HRS

CHEW'S RIDGE EAST-WEST COMPONENT

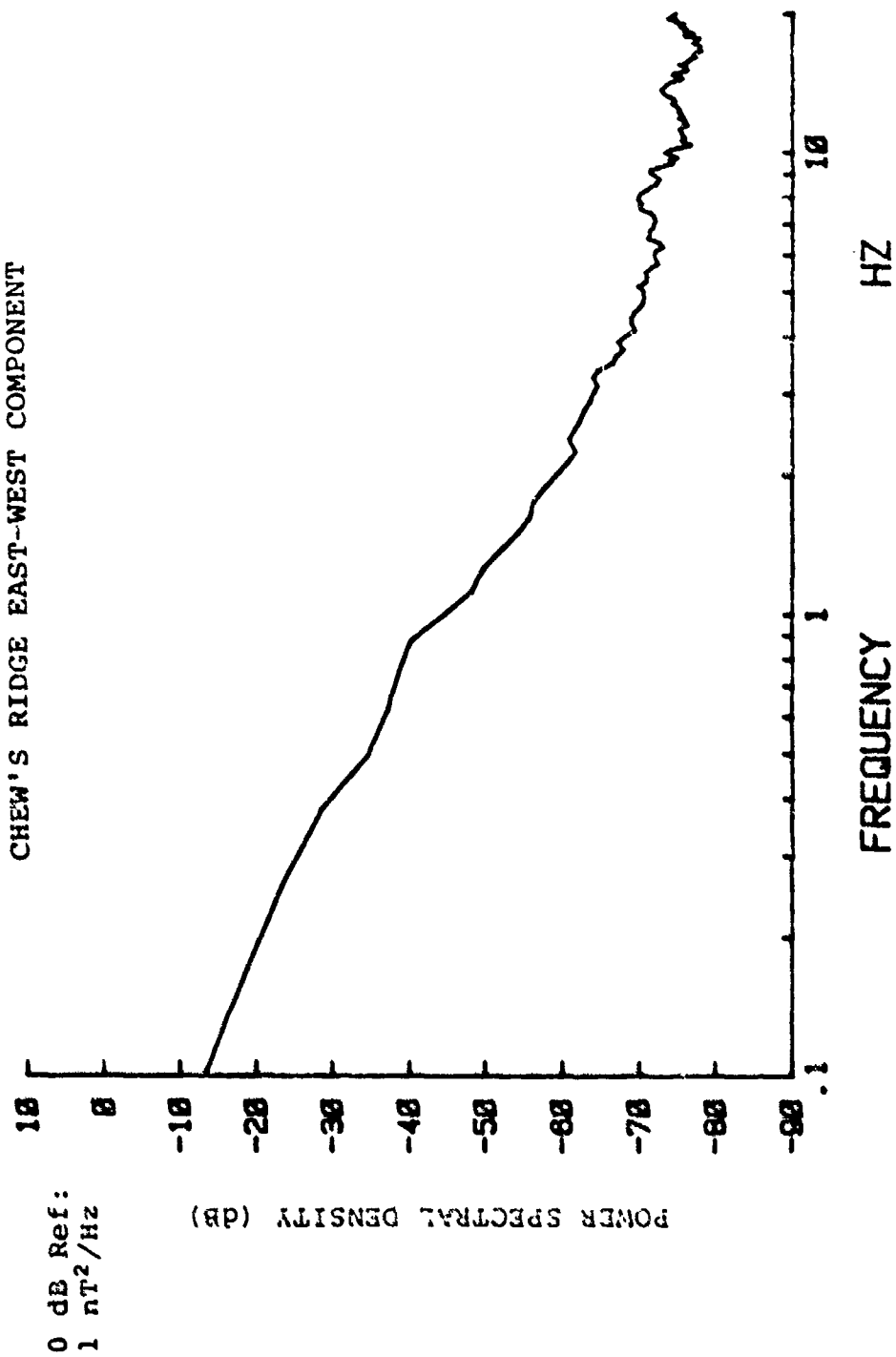


Figure 23. East-West Magnetic Field Fluctuations (.1-20 Hz)

4 OCT 2330 HRS

CHEW'S RIDGE EAST-WEST COMPONENT

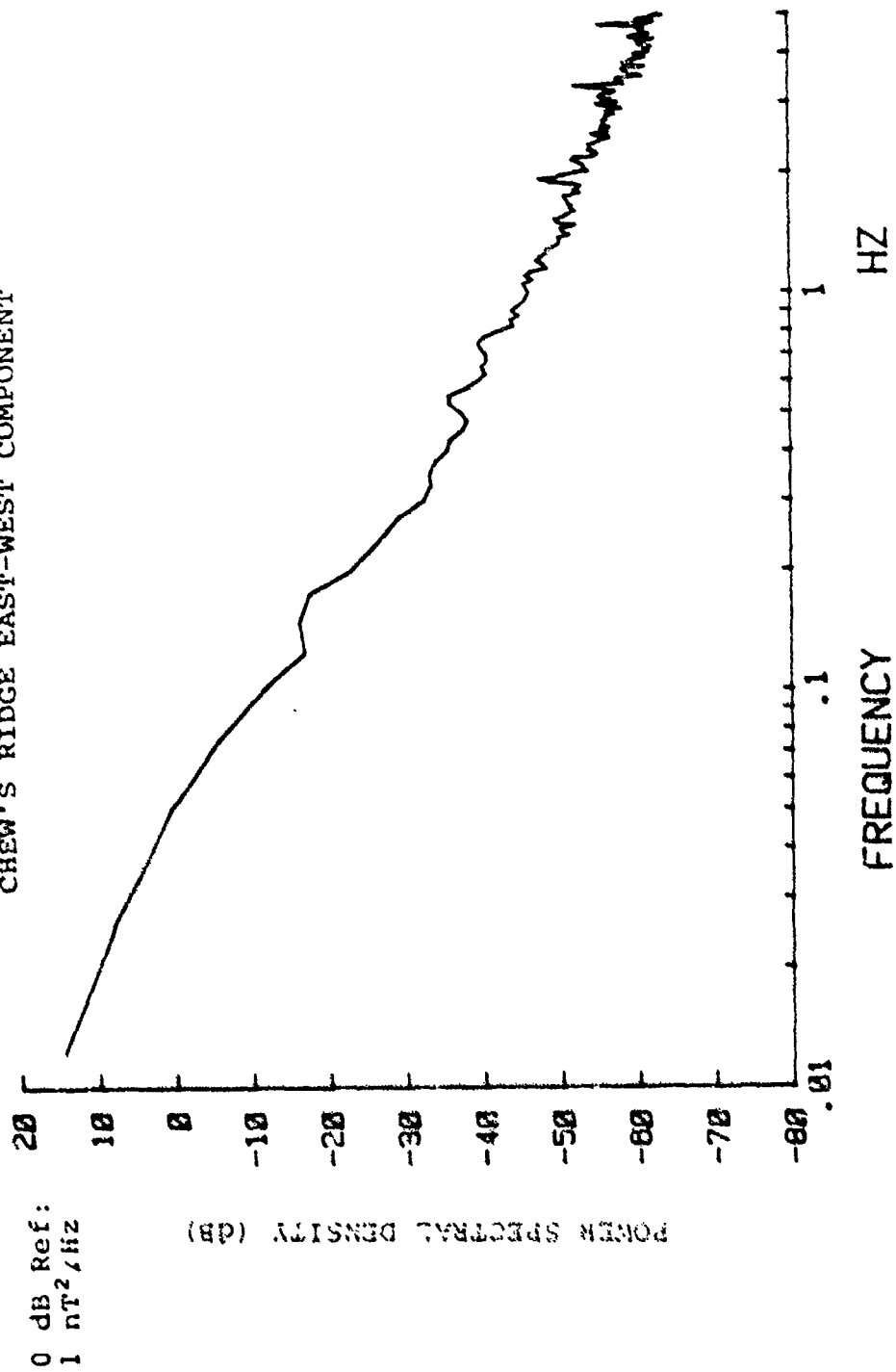


Figure 24. East-West Magnetic Field Fluctuations (.01-5 Hz)

4 OCT 2330 HRS

CHEW'S RIDGE EAST-WEST COMPONENT

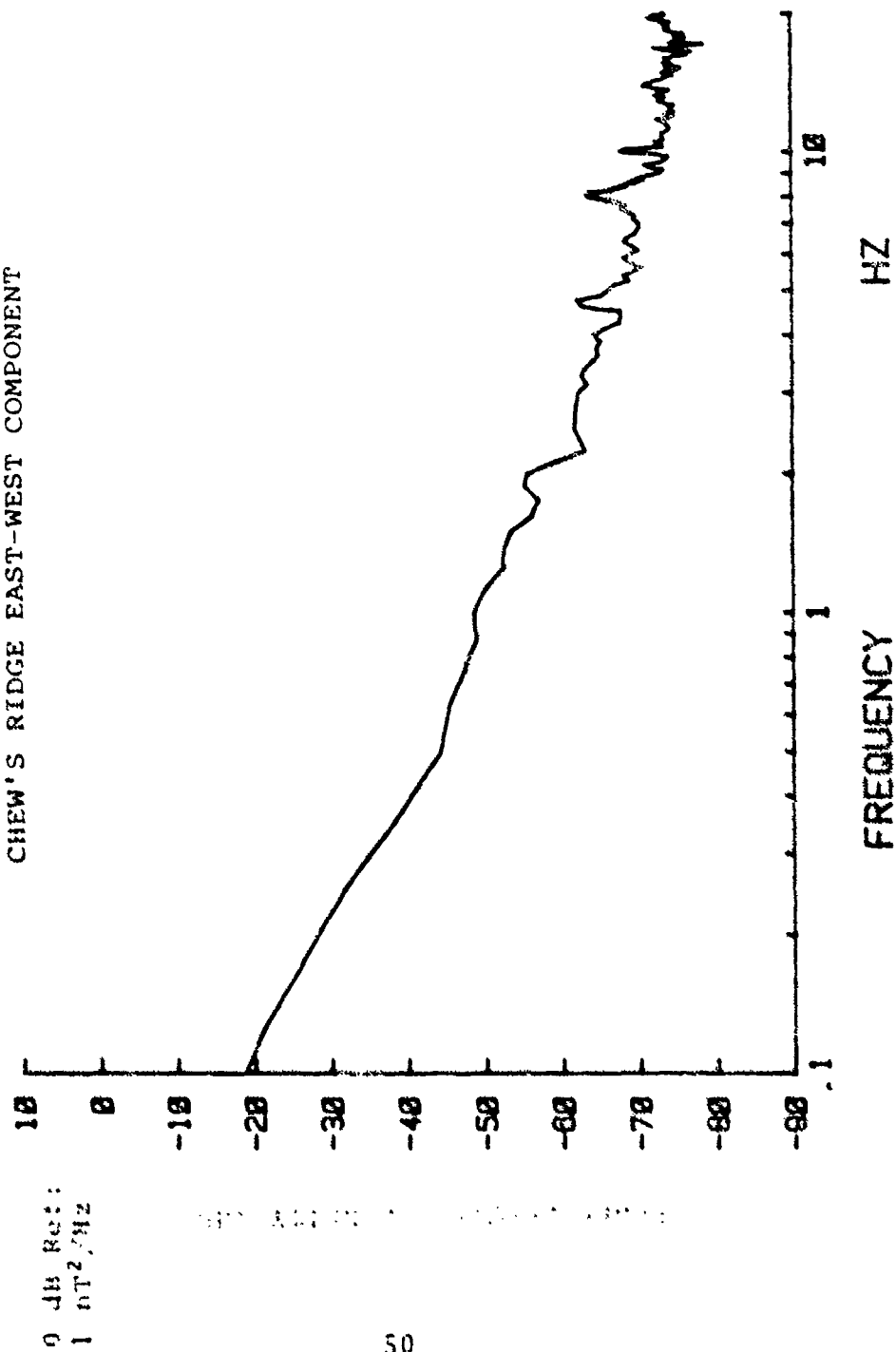


Figure 25. East-West Magnetic Field Fluctuations (.1-20 Hz)

5 OCT 0830 HRS
CHEW'S RIDGE EAST-WEST COMPONENT

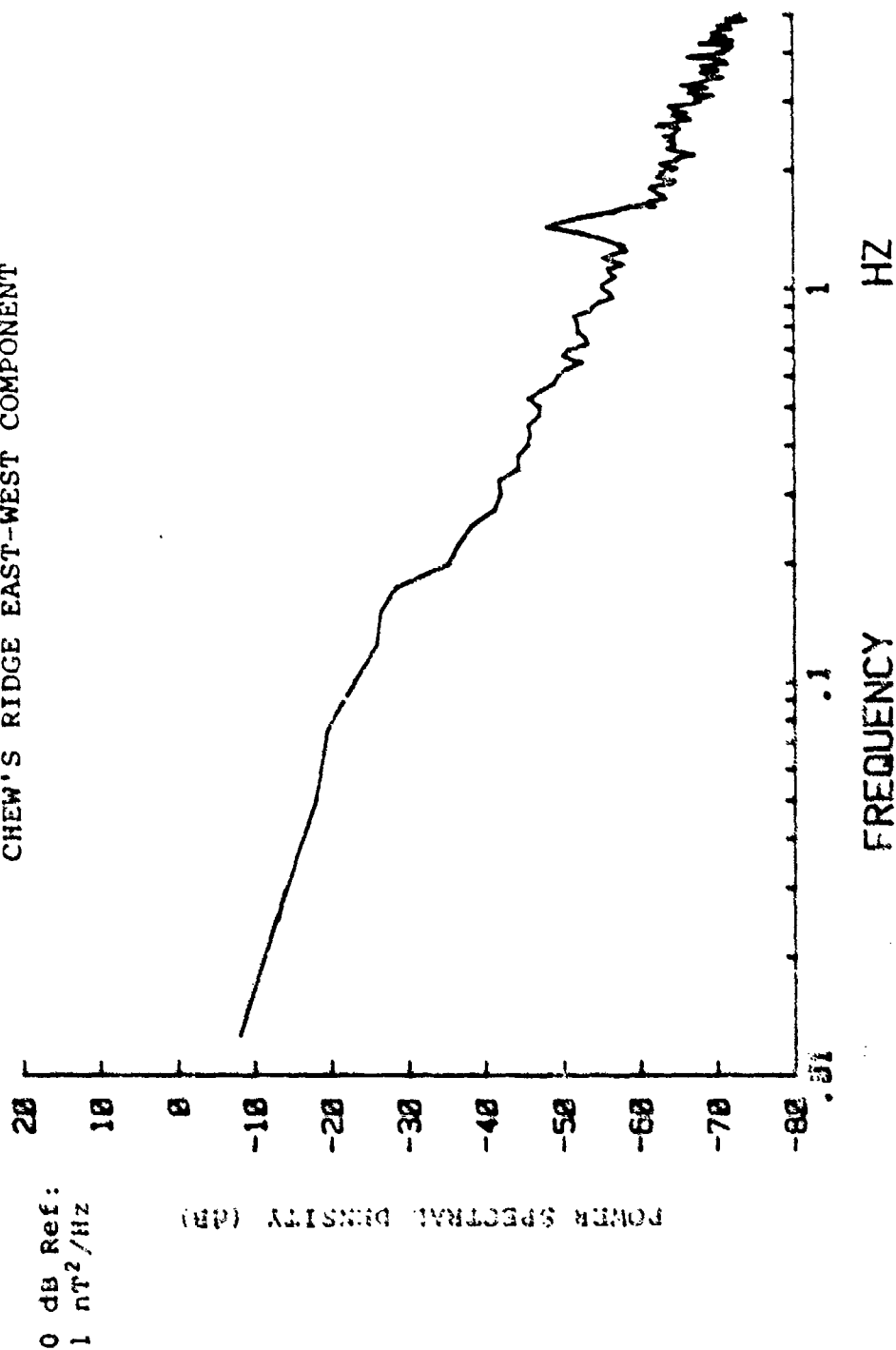


Figure 26. East-West Magnetic Field Fluctuations (.01-5 Hz)

5 OCT 0835 HRS

CHEW'S RIDGE EAST-WEST COMPONENT

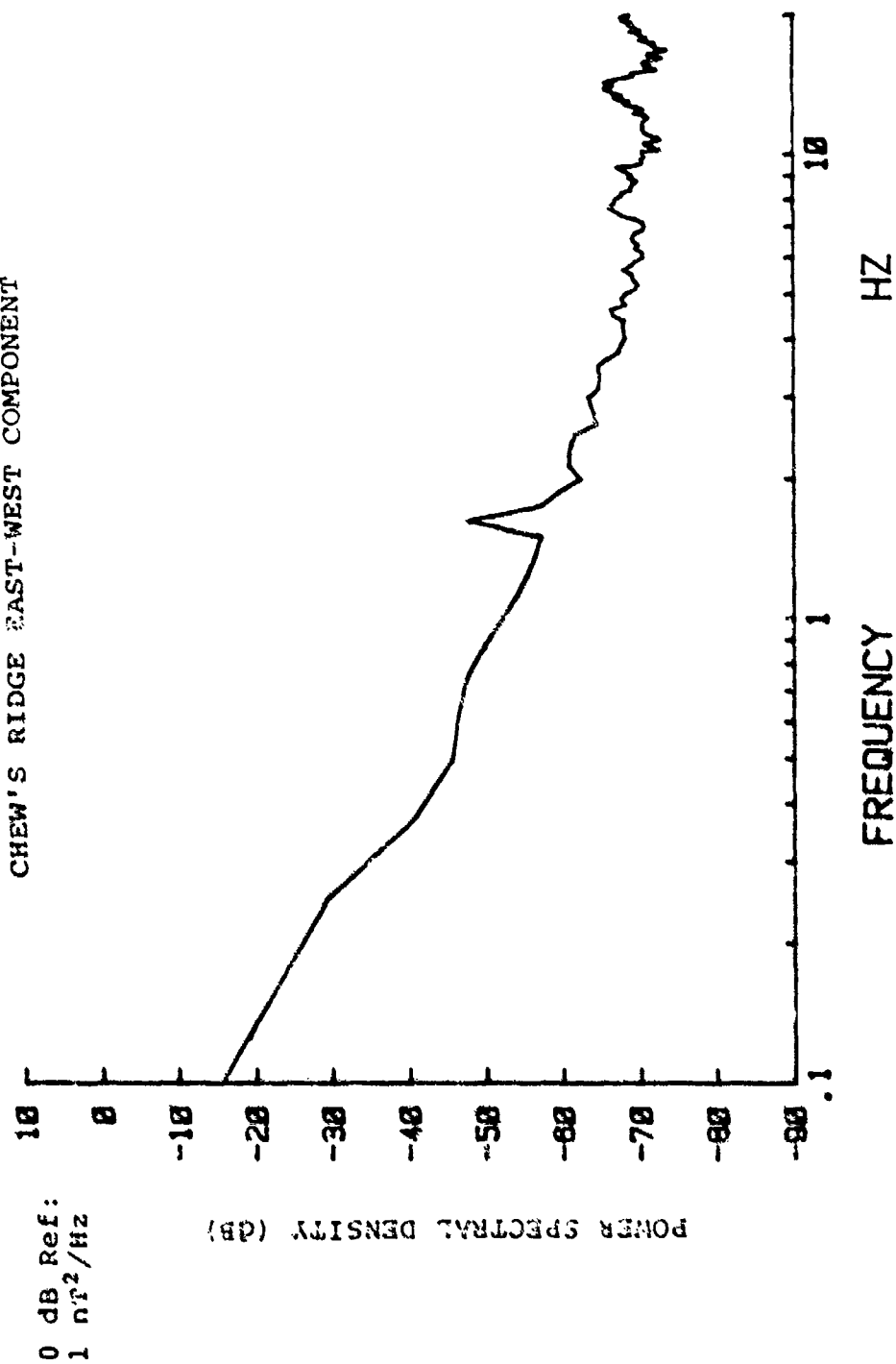


Figure 27. East-West Magnetic Field Fluctuations (.1-20 Hz)

at 0.1 Hz, the average power level drops by roughly 10 dB. An approximate 3 hour lag was also noted after both sunset and sunrise until magnetic activity moved to its normal nighttime and daytime levels. The average East-West spectrum clearly shows the minimum ULF geomagnetic activity in the interval 3-7 Hz as reported by Campbell (1966, 1969) and also by Fraser-Smith and Buxton (1975) in the North-South component. No other minimums were observed in the frequency interval 0.1-20 Hz. In particular, there is no minimum in the frequency interval 0.2-0.5 Hz which separates P₁ geomagnetic pulsations from P₂ (0.1-0.2 Hz) and P₃ (0.022-0.1) pulsations. A minimum of activity could be anticipated near 0.2 Hz because of the very different properties of the P₁ and P₃ classes of pulsations (Jacobs, 1970). Instead, we typically observed a monotonic decrease of activity with increasing frequency throughout the frequency range of .1-3 Hz; however, this could be due to the system's lack of sensitivity at the low frequency end of the spectrum.

The first Schumann resonance, at approximately 8 Hz, produced an increase in the level of geomagnetic activity at frequencies in the range of 6-10 Hz and is clearly seen in the average spectra. Small spectral peaks appear at approximately 2 and 5 Hz during the nighttime hours. These could mark the occurrence of small-amplitude P₁ pulsation events.

CHEW'S RIDGE EAST-WEST COMPONENT

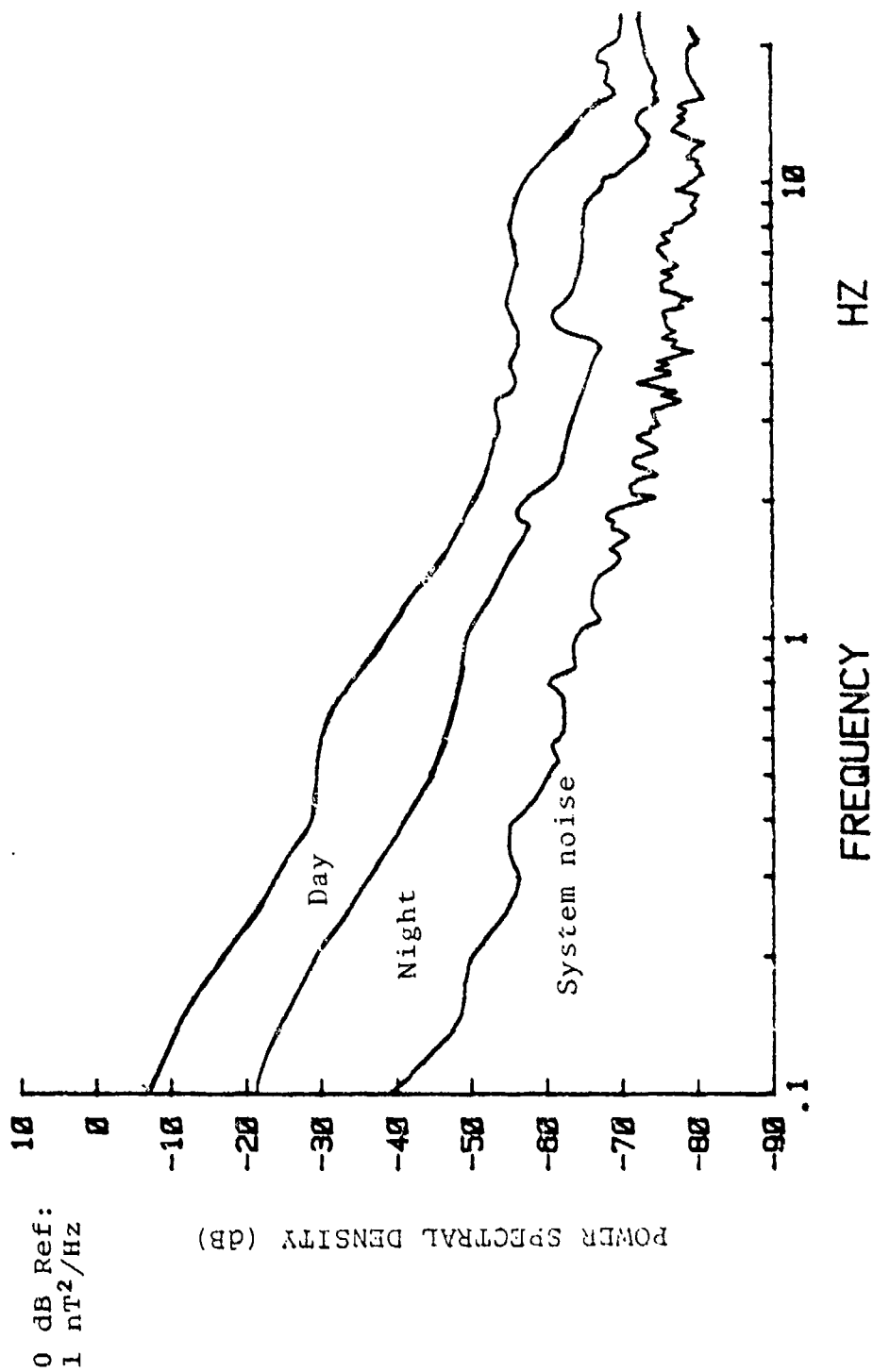


Figure 28. Average Day and Night Power Spectral Density - August-October, 1981

C. OBSERVATIONS AND RECOMMENDATIONS

The prime object of the remote site is to provide a source of reliable data that can be used in support of the Naval Postgraduate School research work on geomagnetic fluctuations on the ocean floor. This required that the data produced by the system during the initial calibration period be checked for consistency with other sources as a measure of its reliability.

A review of previous data taken at Chew's Ridge by Naval Postgraduate School students found one measurement of the East-West component by McDevist and Homan in May, 1980, over the 1-25 Hz frequency range. Measurements made by Fraser-Smith and Buxton (1974) in Stanford, California, approximately 80 miles north of the Chew's Ridge site were also reviewed. The Stanford data was for the North-South component, but was felt to be valid, based upon work by Wertz and Campbell (1976). They found that the North-South and East-West field components were about equivalent in strength at a mid-latitude location $\frac{EW}{NS} = .95$. A third source of mid-latitude East-West horizontal magnetic component measurement was Polk and Fitcher (1962). Each of the three sources gave an average value at .1, 1 and 10 Hz that was within ± 15 dB from the average value of the East-West component obtained from the telemetry system.

A difference of 3-8 dB was also noted between the value obtained at the same frequency when averaged over different

frequency scales. This effect is due to the different amounts of time required to obtain the same number of averages when using the spectrum analyzer - the smaller the frequency range, the greater the time required. An example of this effect is seen in Figures 16 and 17 (25 August, 1981, 0045 hours) where the .1 to 20 scale has a large spike (greater than 15 dB) at approximately 3.1 Hz. The .01 to 5 Hz scale spectra also contain this spike, but it is at least 10 dB and other spikes of nearly equal magnitude have appeared. By watching the instantaneous display on the spectrum analyzer, it was determined that the 3.1 Hz spike was very strong over a four minute period but became much weaker for the next twenty minutes. This indicates an inherent problem of attempting to use spectral analysis methods to evaluate non-stationary processes, such as the earth's changing magnetic field.

While the general behavior of the observed spectra agrees with that illustrated in Figure 3, the amount of data collected during this experiment was not adequate to draw conclusions that could be used as a basis to evaluate underwater data. A longer period of continuous observations, extending throughout the year and for different levels of magnetic activity, is required. A prime object of this effort should be to determine the optimum frequency bandwidth (averaging time) that can be used during different times of the day and at varying magnetic activity levels.

V. EQUIPMENT/SYSTEM IMPROVEMENTS AND RECOMMENDATIONS

The system utilized for the project was subject to numerous breakdowns and was unable to meet the prime objective of providing continuous geomagnetic data.

The main cause of system down time was the overheating of the radio transmitter. Once the maximum operating temperature was exceeded, the radio shut down automatically. Numerous attempts were made to reduce the radio temperature by shading, ventilation and attaching thermal radiators. When none of these attempts proved a deterrent to the overheating, it was concluded that the basic equipment designed by Motorola was the source of the problem. The MX 320 series radio does not appear to have the heat sink capacity necessary to allow rapid radiation of the heat produced during continuous operation; therefore, overheating develops.

The heat problem is compounded by the fact that the 8 volt dc regulated Motorola solar system is designed to vary from 8 to 12 volts dc, according to temperature. These problems have been reported to Motorola and an engineering solution has been requested.

Until an engineering solution is received, the solar system could be disconnected and the radio powered by the storage batteries alone. This would provide a constant voltage of 8.0 volts or less for a period of two weeks at

which time the batteries would be 50% discharged. The batteries could then be recharged by transporting them back to the Naval Postgraduate School or by disconnecting the radio and connecting the solar array to the batteries for charging. This method would allow half time operation (assuming that the radio can operate at a constant 8 volts dc without overheating).

For approximately \$475 an additional 4 batteries could be purchased that would allow almost 100% operation by alternating the charge and discharge of the two systems from 100% to 50%. This method would require bi-monthly maintenance visits to the remote site, a significant increase in maintenance from the original system design.

Another solution would be to design a voltage regulating circuit between the batteries and radio that would allow only 7.5-8.0 volts into the radio. The small difference between the desired voltage and the source voltage makes this difficult to achieve.

Once the solar system voltage fluctuation problem is solved, the system could be further improved by redesigning the VCO and 14 dB amplifier to operate on ± 4 volts dc. This change would allow all of the electronic devices in the storage cabinet to be powered from the storage batteries and two ± 6 volt Gelyte batteries could be eliminated from the system. It should be noted that this change would prevent the VCO and amplifier from being interchanged with those

used in the underwater experiments. At present the theoretical limit to the operating life of the system is the 4 week battery life of the VCO Gelyte batteries. If this modification is made, the theoretical system operating life would be limited by the six month life of the battery powering the preamplifier at the coil. The 14 dB amplifier and the VCO could also be integrated into one chassis, thus eliminating one power connection and enhancing the reliability of the system.

A third improvement could be to increase the area and/or the number of turns in the coil sensors. This would increase the sensitivity of the system, but again, would preclude interchange with the underwater system.

A final area of system improvement could be made in the processing of data. Each graph in this research represents 3-4 man-hours with the majority of time consumed by manually reading the data from the spectrum analyzer and then entering the data, point by point, into the computer for processing and plotting. Since the spectrum analyzer provides the data in a digital format, an interface between the analyzer and the computer should be possible. Perhaps a Hewlett-Packard spectrum analyzer could be obtained with the proper frequency range. In this case the interface problem would be greatly reduced, since the adapters are already in place.

APPENDIX A

EXPERIMENTAL EQUIPMENT AND TESTS

A. EQUIPMENT CONFIGURATION

Most of the equipment utilized in this project was either designed and/or manufactured at the Naval Postgraduate School, while the test and telemetry equipment is mostly of commercial origin. A great deal of the effort expended in this thesis was in testing and ensuring that the experimental equipment operated as conceived and predicted. For example, it is important that all sensor equipment be dc coupled to avoid attenuation of low frequency signals. A discussion of the equipment and its configuration follows:

1. Data Acquisition Equipment

SENSOR

The general hookup of the data acquisition was shown in Figure 5. The sensor is a self-supporting, continuously wound, non-center-tapped coil antenna manufactured by Elma Engineering, Palo Alto, California, from approximately 5460 turns of 18 gauge copper magnet wire. The sensitivity of the coil, as calculated and confirmed by measurement, is given in Appendix B. Its weight is approximately 50 kg. Its overall dimensions (.15m by .37m) are determined by the largest glass sphere that is commercially available. These spheres are used to enclose the coil during underwater experiments. The

coil resistance is 124 ohms and its self-inductance is approximately 9.31 henries.

PREAMPLIFIER

The differential preamplifier Model 13-10A is an improved version of Model 13-10 which was employed by McDevitt and Homan (1980). This preamplifier was selected because of its low power requirements, compactness and excellent low frequency noise characteristics. The final stage of the preamplifier also contains an active filter which provides a sharp cutoff for frequencies above 20 Hz. The overall preamplifier gain for inputs of less than 2.5 millivolts is 60 dB. The preamplifier is buried with the sensor coil at the test site. It is connected to the rest of the system by 90 meters of armored cable, for rodent protection. Both ends of the cable are protected by diodes to prevent large voltage surges due to lightning from entering the system. An additional 14 dB amplifier was placed at the end of the cable to provide an average voltage range of 0-10 millivolts into the VCO. A graph of the overall amplifier gain characteristics is included as Figure 29. A schematic diagram of the preamplifier circuit is shown in Appendix C.

VOLTAGE CONTROLLED OSCILLATOR

A schematic diagram of the voltage controlled oscillator (VCO) is included in Appendix C. The function of the VCO is to convert low frequency analog voltages received

PREAMPLIFIER GAIN CHARACTERISTICS

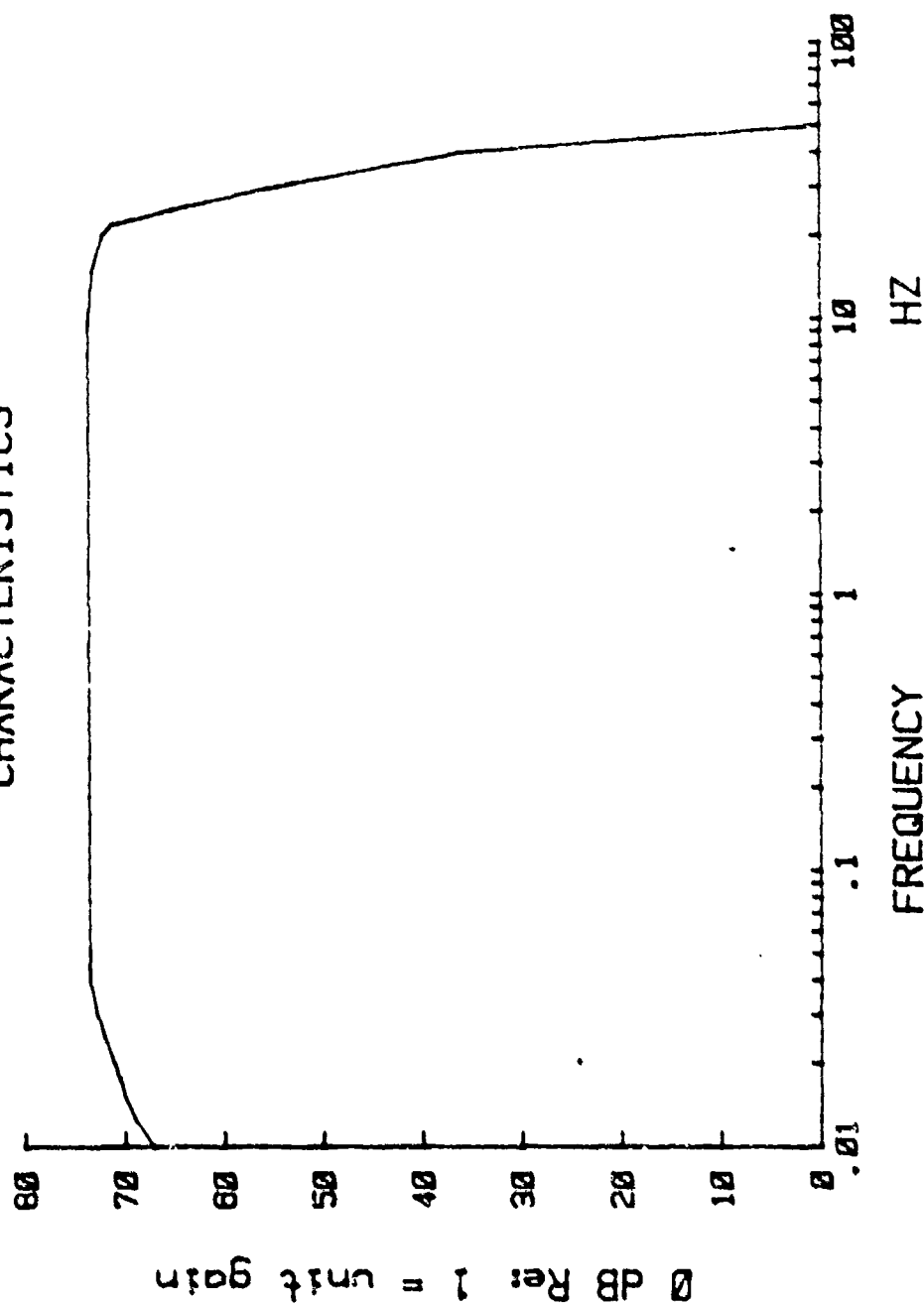


Figure 29. Amplifier Gain Characteristics

from the sensor through the preamplifier into a time varying frequency, centered at 1500 Hz. The output level of the VCO is approximately 0.4 volt (zero to peak) square wave of varying frequency which is then transmitted by the telemetry system. The conversion factor for the VCO is 50 Hz/mV.

SITE TRANSMITTING EQUIPMENT

An MX Portable 302 series (Motorola Model H23AAU1120N) two channel radio had been selected for utilization at the monitoring site, (Beliveau, 1980). It has an output power of 1 watt, RF bandwidth of 16 KHz, and a channel spacing of 25 KHz. It is designed to operate at 7.5 volts. This radio required modification to operate in the continuous mode for telemetry data transmission. A Motorola vehicular antenna adapter cable (Part No. NKN-6223) was added to allow the use of an external antenna. A Motorola external microphone speaker (Part No. NMN-6070) also was installed. This allowed the radio to be operated for voice transmission or switched to continuous transmission of the VCO output signal.

A six element Yagi antenna, DB-292 (manufactured by Decibel Products, Inc.) Was selected for use with the radio. The antenna consists of a reflector, driven element (folded dipole), and four directors mounted on a common support boom. Gain and VSWR are essentially constant (maximum gain of 9.5 dB at mid frequency) across a 10 MHz band (providing optimum performance if a multi-frequency system is later installed). The DB-292 has a beamwidth of 50 degrees.

2. NPS Receiving Equipment

Another Yagi antenna was mounted on the roof of Spanagel Hall at the Naval Postgraduate School. The antenna, also by Decibel Products, Inc., is a DB-292-2 (2 stack array) providing a 12.1 dB gain.

A 40 watt output power, two channel, base station (Motorola Model L4355B1136) is the transmitter/receiver at Spanagel Hall. It has a receiver sensitivity (with preamplifier) of 0.25 microvolts and an output impedance of 50 ohms. This yields a receiver sensitivity of -199 dB_M . Comparing this receiver sensitivity to the minimum monthly median signal level expected (as calculated by Beliveau, 1980), yielded a signal excess of about 40 dB.

PHASE LOCK LOOP

Radio waves are affected by many factors during their travel from transmitter to receiver. Factors such as frequency, distance, antenna heights, curvature of the earth, atmospheric conditions, and the presence of intervening obstacles such as hills, buildings, and trees all enter into the calculation of the total loss of the propagation path. Each radio system has a maximum allowable transmission loss which, if exceeded, results in poor or total loss of reception.

The Chew's Ridge to Naval Postgraduate School transmission is subject to random bursts of static noise superimposed on the audio data tone. These static bursts

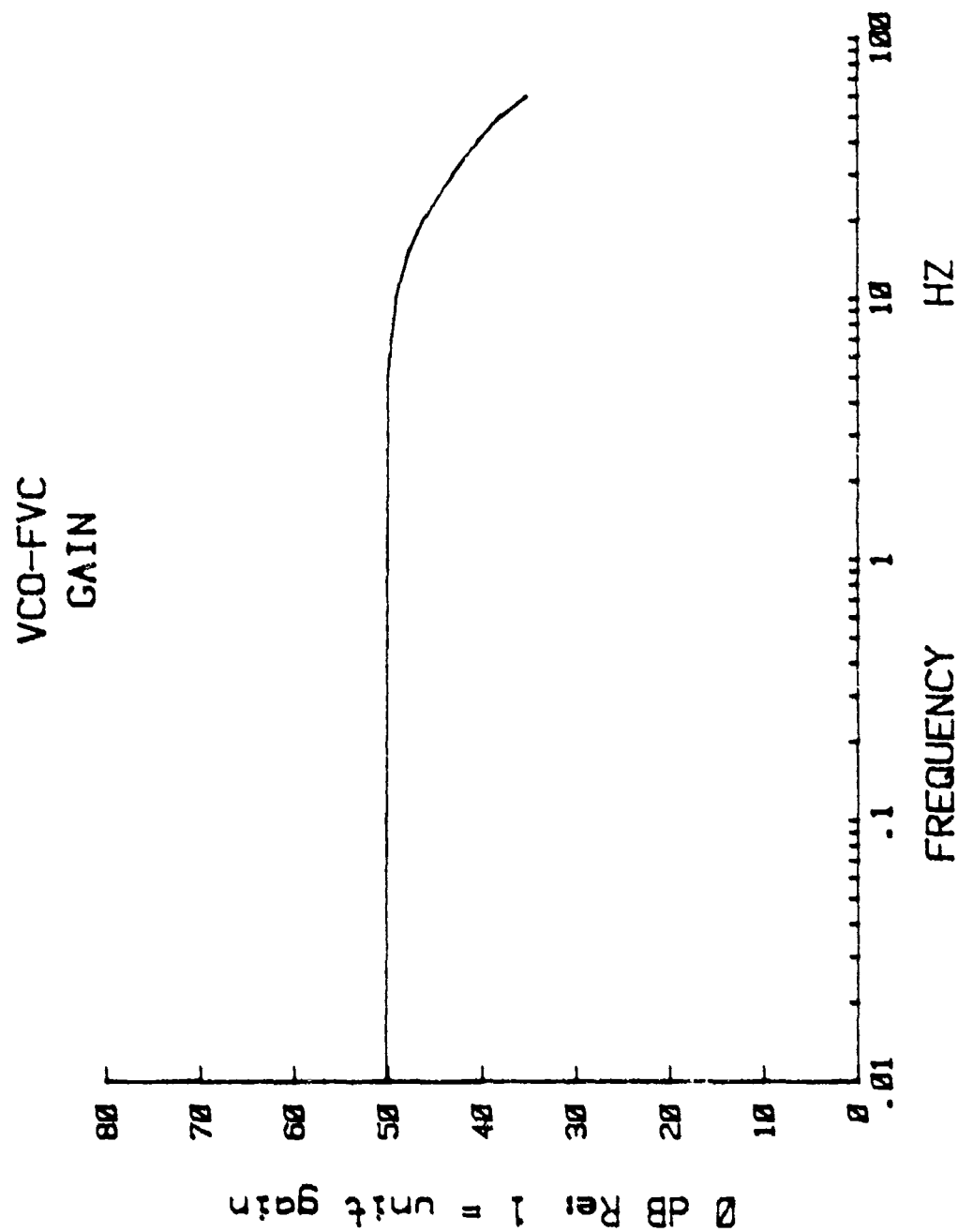


Figure 30. VCO/FTV Gain Characteristics

2. NPS Receiving Equipment

Another Yagi antenna was mounted on the roof of Spanagel Hall at the Naval Postgraduate School. The antenna, also by Decibel Products, Inc., is a DB-292-2 (2 stack array), providing a 12.1 dB gain.

A 40 watt output power, two channel, base station (Motorola Model L4355B1136) is the transmitter/receiver at Spanagel Hall. It has a receiver sensitivity (with pre-amplifier) of 0.25 microvolts and an input impedance of 50 ohms. This yields a receiver sensitivity of -119 dB_M. Comparing this receiver sensitivity to the minimum monthly median signal level expected (as calculated by Beliveau, 1980), yielded a signal excess of about 40 dB.

PHASE LOCK LOOP

Radio waves are affected by many factors during their travel from transmitter to receiver. Factors such as frequency, distance, antenna heights, curvature of the earth, atmospheric conditions, and the presence of intervening obstacles such as hills, buildings, and trees all enter into the calculation of the total loss of the propagation path. Each radio system has a maximum allowable transmission loss which, if exceeded, results in poor or total loss of reception.

The Chew's Ridge to Naval Postgraduate School transmission is subject to random bursts of static noise superimposed on the audio data tone. These static bursts create

numerous high frequency components and degrade the system's ability to reduce the data to meaningful information.

A phase-lock loop was designed to track the 1500 ± 500 Hz audio signal and to filter out sudden random static frequencies.

The loop parameters are:

1. Equivalent loop noise band width 500 Hz
2. A damping ratio of $1/2$.

TAPE RECORDER

The tape recorder employed for this project is a Hewlett-Packard model 3960 Series Instrumentation Tape Recorder. The tape speed was $3 \frac{3}{4}$ ips. Additional characteristics, for this tape speed, are:

1. Frequency response: 50 Hz - 15 KHz
2. Signal-to-noise ratio: 38 dB
3. Flutter % peak to peak: 0.4

Flutter compensation is incorporated in the recorder to compensate for any flutter component introduced by tape speed variations. When the flutter compensation switch located behind the access door on the upper left frame of the chassis is set to "On", channel 2 cannot be used for data recording. During reproduction, the output of channel 2 is inverted (phase changed by 180°) and added to the other FM channel, thereby cancelling the flutter in these channels.

Other systems in use at the Naval Postgraduate School employed portable cassette type tape recorders that are operated while sealed in glass spheres at depths of up to 300 feet below the ocean surface. To reduce WOW and flutter in these recorders, a 2 KHz reference oscillator signal is recorded simultaneously with the VCO data signal, and the difference frequency is then the input to the frequency-to-voltage converter. The reference and data signals are mixed on playback. This method was tried but showed no improvement relative to results obtained with the HP 3960 with flutter compensation.

FREQUENCY-TO-VOLTAGE CONVERTER (ANADEx PI-375)

The purpose of the frequency-to-voltage converter (FVC) is to convert the frequency difference from the standard 1500 Hz VCO output into an analog voltage. The varying voltage is then a representation of the geomagnetic fluctuations detected by the sensor. The FVC is powered by 24 Vdc and has the following additional characteristics:

1. Input frequency range: 500-5000 Hz
2. Output dc voltage: 0-8 volts full scale
3. Conversion factor: 5 mV/Hz

The conversion factor depends upon the amount of dc offset introduced by the FVC. The greater the offset, the greater the mV/Hz sensitivity. The sensitivity possible is limited by the need to keep the response linear over the frequency

range expected. The output of the FVC is then analyzed with a spectrum analyzer. A graph of the VCO-FVC gain characteristics is Figure 30.

SPECTRUM ANALYZER (S/A)

A Mini-Ubiquitous Model 400 was employed for spectral analysis. It allows for dc coupling, has a digital display of the power spectrum, and has a logarithmic, as well as a linear frequency scale.

Since the discriminator output is a positive dc voltage, it is necessary to provide for a dc offset in order to increase the input sensitivity of the spectrum analyzer. A Textronic Model AM 502 differential amplifier was used to remove the dc offset.

POWER SUPPLIES

1. Batteries

Gould Gelyte batteries have been utilized to meet the dc power requirements of the preamplifiers and the voltage controlled oscillator. They are sealed, rechargeable, and virtually maintenance free batteries, containing no free electrolyte. The preamplifier is powered by two 12 Vdc 18 ampere-hour batteries providing \pm Vdc. The 14 dB amplifiers and the VCO are powered by two 6 Vdc 18 ampere-hour batteries providing \pm 6 Vdc. These batteries require replacement and recharging approximately every three months.

The MX 320 radio is powered by 4 low discharge lead-acid batteries (Willard Type DH-5-1) connected in series to provide 8 volts. Each battery provides 600 amp-hours at 77° at 2 volts. Since the geomagnetic data is transmitted continuously (100 % duty cycle), the battery system is designed to allow for about 28 days operation without recharging. This is based upon a power requirement of 22.1 amp-hours per day (19.2 amp-hours with a 15% safety factor). The batteries would then be completely discharged and require replacement.

2. Solar Array

The purpose of the solar array is to provide an 8 volt source to recharge the continuously discharging batteries. Since the array output will vary depending upon the sunlight available, an 8 volt regulator is utilized to prevent battery damage due to charging voltages higher than 8 volts. This 8.0 volt rating is a nominal voltage rating and the actual voltage output will vary from 9 to 11 Vdc depending on the thermistor temperature. The thermistor is a remote assembly that senses the ambient temperature in the vicinity of the storage batteries and determines the desired output voltage of the regulation.

In addition, a separate low voltage Schottky diode is incorporated in the regulator to prevent battery discharge through the solar array during non-sunshine periods. The solar array/battery arrangement is designed for continuous operation on the basis of 8 sunless days. The absence of

sunlight beyond the 8 day limit will lead to system shut-down and battery replacement or recharging.

The solar panels (MSP43A40, Motorola Solar Systems) consist of a series of photo-voltaic cells each providing a specific voltage per cell depending upon the amount of sunlight available for the conversion of light energy to electrical energy. The array consists of two modules in parallel. The array was faced toward true south at a slope of 47 degrees from the horizontal in order to capture the maximum amount of sunlight as the earth revolves and the sun "moves" from the eastern to the western horizon. The amount of total energy can be greater if the angle is changed to 61° in the winter and to approximately 45° in the summer. In general, the months of November, December, and January will have the lowest system output to load ratio since the temperature will be seasonally low creating a higher rate of discharge (poor battery efficiency). The daylight is also shorter during these months, resulting in less sunlight captured by the solar array. Table 1 shows the predicted system performance for the various months of the year.

MONTH	MWH/SQCM PER DAY ON HORIZONTAL	MWH/SQCM PER DAY ON ARRAY	*ARRAY OUTPUT AMP-HRS PER DAY	LOAD AMP-HRS PER DAY	*ARRAY OUTPUT TO LOAD RATIO	*SYSTEM OUTPUT TO LOAD RATIO
JAN	216	369	18.58	19.20	.97	1.23
FEB	343	505	25.58	19.20	1.33	1.42
MAR	508	591	30.11	19.20	1.57	1.83
APR	633	550	28.14	19.20	1.47	2.02
MAY	740	516	26.48	19.20	1.38	1.93
JUN	809	506	26.02	19.20	13.6	1.91
JUL	776	510	26.19	19.20	1.36	1.92
AUG	704	556	28.51	19.20	1.48	2.04
SEP	584	608	31.00	19.20	1.61	2.17
OCT	435	611	31.01	19.20	1.62	2.17
NOV	280	482	24.32	19.20	1.27	1.82
DEC	185	330	16.54	19.20	.86	1.41

ARRAY SAFETY FACTOR = 35.6% ANNUAL, -13.8% WORST-MONTH

*INCLUDES 15% SAFETY FACTOR

*SYSTEM OUTPUT = ARRAY OUTPUT + AVAILABLE SEASONAL BATTERY CAPACITY

Table 1. Predicted Power Supply Performance

A. SENSOR SENSITIVITY

1. Theoretical Sensor Sensitivity

Faraday's Law of Induction shows that the electromotive force (emf) induced in a single-turn circuit is equal to minus the rate of change of flux.

$$\text{emf} = -\frac{\partial \Phi}{\partial t}$$

Where the flux passing through a surface bounded by the conductor is defined as:

$$\Phi = \int \vec{B} \cdot d\vec{A}$$

For N turns of wire connected in series, the total emf induced is the sum of the emf induced in each separate loop:

$$\text{emf} = -N \frac{\partial \Phi}{\partial t}$$

Assuming that magnetic fields vary sinusoidally with time and may be written as:

$$\vec{B} = \vec{B}_0 e^{-j\omega t}$$

Where \vec{B}_0 is a magnetic vector field that is only a function of spatial coordinates and not of time. Therefore we have:

$$\text{emf} = -NB_z j\omega A$$

Where A is the area of the coil and B_z is the axial component of \vec{B}_0 .

The magnitude of emf is

$$\text{emf} = NB_z (2\pi f)A$$

Since the output of the sensor is connected to a high input impedance amplifier, then negligible current can flow through the sensor which might otherwise produce a back emf and reduce the magnitude of the field to be measured. The sensor's open circuit voltage or sensitivity can be calculated for the coil parameters given in Appendix A for a 1nT field at a frequency of 1Hz; $\text{emf} = 2.8316 \mu\text{V}$, therefore $20 \log(\text{emf}) = -110.95 \text{ dB}(\text{re: } 1 \text{ volt})$.

The area used for the calculation was the average of the areas found by using the inner radius and outer radius of the coil.

2. Experimental Determination of Sensor Sensitivity

As was found by McDevitt and Homan, (1980), the need for a uniform magnetic test field required the use of a .61 meter radius Helmholtz coil. The Helmholtz coil produced a known field at a specified distance and the electromotive force produced by the sensor was then measured. The coil is designed to produce an easily accessible, almost homogeneous magnetic field in the central region between the coils.

Expressions for the magnetic induction vector for the axial and radial components are:

$$B_z = \frac{\mu_0 8NI}{5 \cdot 5 R} \left[1 - \frac{144}{125} \frac{Z}{R} + \frac{54}{125} \frac{Z^2 r'^2}{R^4} + \dots \right]$$

$$B_{r'} = \frac{\mu_0 8NI}{5 \cdot 5 R} \frac{12Zr'}{125 R^4} (3Z^2 + 10r'^2 +)$$

as given in (Jefemenko, 1966).

Therefore, in the central region

$$B_z = \frac{8NI}{5\sqrt{5} R}$$

$$B_{r'} = 0$$

to the terms of the order (L/R) where L is the linear dimension of the region. Specifying the desired field strength and distance determines the current through the coil at different frequencies. To produce the required current, a variable resistor was placed in series with the coil and the signal voltage was set according to:

$$V = I(R_1 + R_2)$$

Where R_1 = coil impedance

R_2 = variable resistor

The current was determined to be within $\pm 1.0\%$ of one mA and the field produced along the central axis of symmetry was determined to within $\pm 10\%$ of a nT. The main reason for the slight difference in sensor sensitivity obtained from that of McDevitt and Homan was the use of $N = 5460$ turns versus $N = 6000$ turns, where the first was the actual count obtained from the manufacturer.

B. PREAMPLIFIERS, VCO, AND FVC

Once the sensor sensitivity had been verified using the Helmholtz coils, the other gains and conversions of the electronic component were determined. This was done by inputting a known signal at varying frequencies to each component and measuring the output.

The major problem encountered was producing the stable calibrated known signal. The source used for the final calibration was a Hewlett-Packard 3320B Frequency Synthesizer. The main reason for its selection was the output level control range of +26.99dB to -69.99dB. This allows the input to the preamplifier to be in the 1-2 milli volt range.

The outputs are then measured by oscilloscopes and the gains calculated.

C. SPECTRUM ANALYZER

The spectrum analyzer, when in the dBV display mode read:

$$N(\text{dBV}) = 20 \log \frac{A \text{ volts}}{1 \text{ volt}}$$

Since 0 dB referenced to 1nT not 1 volt is desired:

$$\left(\frac{A \text{ volts}}{1 \text{ volt}} \right) \left(\frac{X \text{ volts/nT}}{X \text{ volts/nT}} \right) = \left(\frac{A \text{ volts}}{X \text{ volts/nT}} \right) \left(\frac{X \text{ volts}}{1 \text{ volt nT}} \right)$$

Where B (the field measured by the system) is:

$$B = \left(\frac{A \text{ volts}}{X \text{ volts nT}} \right)$$

THEORETICAL SENSOR SENSITIVITY 1 mT FIELD

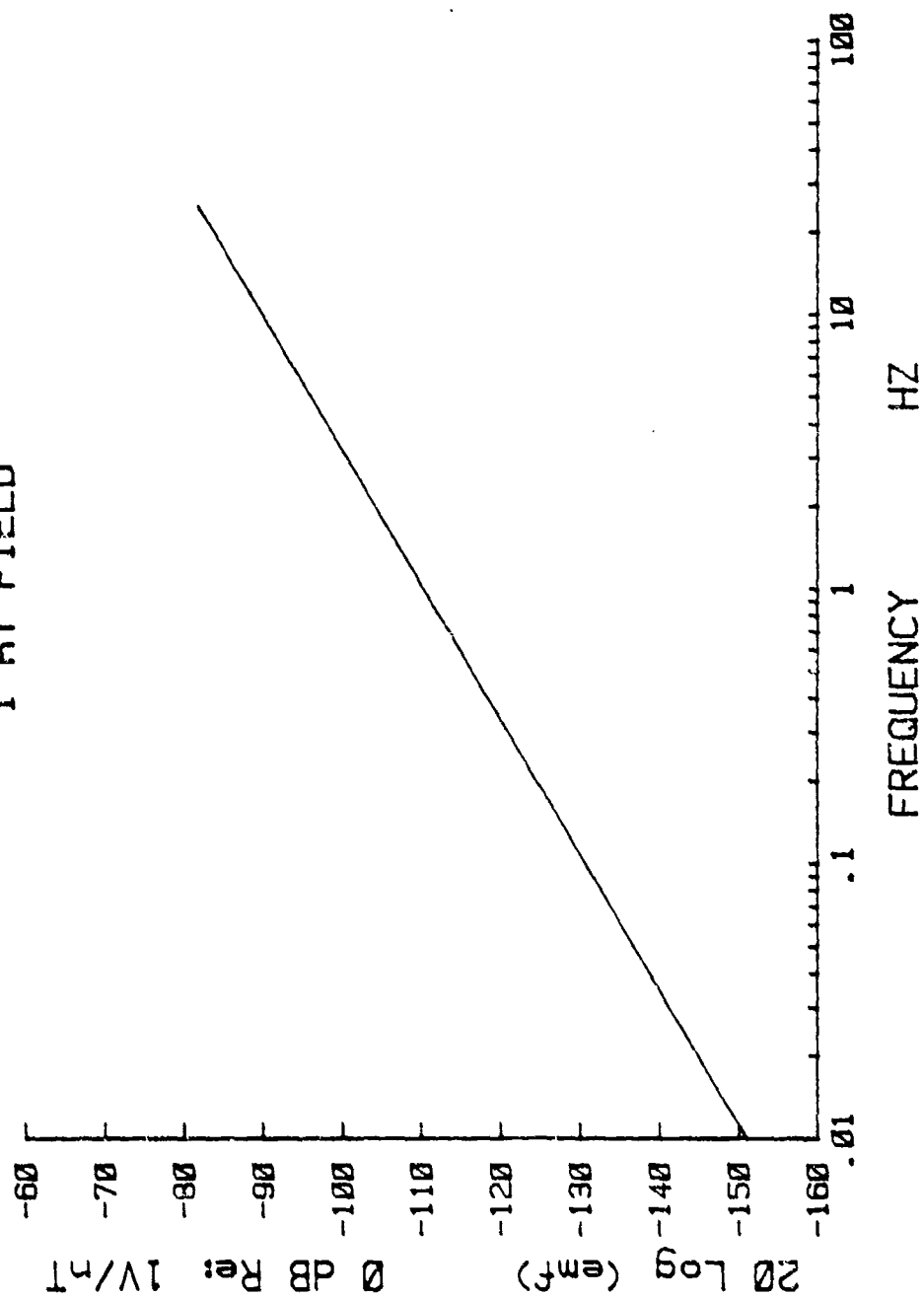


Figure 31. Theoretical Sensor Sensitivity

so referenced to $\ln T$ we have:

$$N(\text{dB}) = 20 \log \frac{B}{\ln T} + 20 \log X$$

where X is the system transfer function given in units of volts/ $\ln T$.

Since spectrum analyzers use various averaging windows and have various numbers of bins, the following corrections must be applied:

$$B^2 = \Phi(BW).$$

$$\text{and } (BW) = \left(\frac{\text{frequency range}}{\text{number of bins}} \right) (\text{window corrections})$$

Therefore

$$N(\text{dB}) = 20 \log [\Phi^{1/2}(BW)^{1/2}] + 20 \log X$$

or

$$10 \log \Phi = N(\text{dB}) - 20 \log X - 10 \log (BW)$$

where $10 \log \Phi$ is the corrected reading or the power spectral density. Φ has the units of nT / Hz .

For the Mini-Ubiquitous Model 440, the window correction is 1.5 dB and it uses 400 averaging bins. The BW correction on the 0-20 Hz scale was:

$$BW = \left(\frac{20}{100} \right) (1.5) = 0.075$$

$$-10 \log BW = 11.25$$

APPENDIX C
EQUIPMENT SCHEMATICS

Figure 33 shows the preamplifiers utilized in this project. It is an improved low noise ELF amplifier model 13-10A designed to provide the quietest operation, i.e., greatest signal-to-noise ratio. Figure 34 is the VCO unit used in this system.

APPENDIX D
EQUIPMENT USAGE AND MAINTENANCE

The equipment utilized in this system requires a certain amount of periodic maintenance and handling. Below is a list of hints and suggested activities which might help to prevent equipment damage and prolong the life of the system.

A. REMOTE SITE EQUIPMENT

The first action upon arrival at the remote site should be to open the storage cabinet and inspect the radio, VCO, storage batteries and solar system. (Note: Opening the storage cabinet requires a 3/8 inch socket to remove counter sunk lag bolts holding the access panel.)

1. Willard Charge Retaining Batteries Type DH-5-1 require the addition of water once a year under normal operations. If the solar charging panel voltage is providing more than 9.2 volts, gassing may occur and more frequent water addition may be required. The electrolyte level should be 1 3/4 inches (4 cm.) above the battery plates. The state of charge may be checked by using a hydrometer to measure the specific gravity of the electrolyte. The hydrometer used should have a float calibrated to read lower than the standard automotive type hydrometer. A fully charged cell will have a specific gravity reading of 1.300, while a discharged cell will read 1.075. The cut-off voltage is 1.75 volts per cell or a system voltage of 7 volts.

The storage batteries supplied with the system contain a strong acid electrolyte. The following general precautions for the safe handling of the storage batteries should be observed:

a. In the operation of an acid battery, hydrogen gas is liberated which may be explosive if ignited. The battery area should be checked for signs of hydrogen gas build-up (particularly at the ceiling) prior to performing any electrical checks that could be spark-producing.

b. Plastic or rubber gloves, an apron and safety goggles should be worn if the batteries require handling. Fresh water should be available so that the electrolyte can be rinsed off immediately if it comes in contact with the skin. A mixture of 1 pound bicarbonate of soda in one gallon of water can be used to neutralize acid spills. Apply the solution until bubbling stops, then thoroughly rinse the area with water.

c. When diluting an electrolyte, always add the electrolyte to water slowly, with constant stirring. Explosive reactions can occur if water is added to the electrolyte.

2. Solar Systems

It is recommended that period maintenance on the solar system be performed annually during the springtime. The advantage of springtime maintenance lies in its benefit to the storage batteries. If water additions are required, the battery electrolyte level will be topped off just before

entering the season of greatest water usage - summer. As water is consumed, the proportional acidity of the electrolyte level will increase and will achieve its highest level during the winter months, providing additional freeze protection.

The minimum yearly required solar array maintenance is listed below:

a. Inspect the solar modules for dirt, dust, bird droppings, insects or other foreign material on the glass. Clean with warm water and a soft cloth as necessary.

b. Inspect the module mounting and anchor bolts for tightness and tighten as necessary.

c. Inspect the silicone weatherization and leads of each module for adequate weatherization. Tighten the terminals and repair the silicone weatherization as necessary.

d. Inspect the wiring insulation for cracking, peeling or other defects. Replace as necessary.

e. Inspect the installation site for any new growth of weeds, shrubs, trees, etc., which have obscured the exposure of the solar array to the sun and which may have caused localized shading of the array. Inspect the voltage regulator for bird or rodent nests also. All such obstructions should be removed or cleared as necessary.

f. Note the ambient temperature in the vicinity of the thermistor housing. Using a voltmeter capable of 2% accuracy at the measured voltage, check the voltage between

the positive battery terminal and the negative battery terminal. The reading should be between 9.1 and 10.3 volts dc.

g. If the voltage is lower than 9.1, the batteries should be disconnected and the voltage measured again. It should now be within the prescribed limits. (Explanation: If the battery is fully charged and the solar array is generating its full output, the regulator will be operating to clamp the battery voltage at the level required for the particular battery temperature. If the battery is accepting a substantial charge current however, the output voltage will be lower and it will be necessary to disconnect the battery to force the regulator into operation.

h. If the voltage is high, or if it is low even with the battery disconnected, the thermistor control needs readjustment. If this is the case, the regulator should be returned to the factory for adjustment.

i. Next, measure the short circuit current of the array using a current meter with a sufficiently low internal resistance (i.e., its terminal voltage). Disconnect the array from the battery and connect the ammeter across the two levels. When disconnecting the meter after the reading is taken, the connection should be broken rapidly since there will be a tendency to draw an arc and burn the leads. The short circuit current reading should be greater than 4.0 amperes.

3. Antenna

Maintenance of the field antenna consists of checking the weatherization of the cable connections between the radio and the antenna, insuring that the anchoring system is tight and verifying that the antenna is properly aligned with the base station.

4. Electronic Equipment

The particular concern with the electronic equipment is the proper application of the power supply voltages. Improperly applied voltages may result in integrated circuit and/or printed circuit board damage. The most likely time for this to occur is during the replacement of the Gelyte batteries that power the VCO and Preamplifier. The suggested application of dc power is to first, connect the non-common (+) leads, being certain to observe the correct polarities; then, connect the common lead, being careful not to short the common lead against the equipment chassis. Circuit power should not be applied unless there is a load on the input. During normal maintenance the following sequence is recommended:

- a. Open the equipment storage cabinet and allow any build up of battery gas to displace while checks and service of the solar array and antenna are performed.

- b. Disconnect the VCO from the radio and use headphones to monitor the sensor signal coming from the VCO. If

the signal is the characteristic wavering 1500 Hz centered tone, the system is operating normally and only battery replacement and normal housekeeping are required. If, on the other hand, the signal is steady, centered well away from 1500 Hz or there is no signal, each component from the VCO to the coil must be checked for proper operation. A Simpson Model 260 volt-ohmmeter or its equivalent is helpful in isolating the source of failure.

c. For normal service, the next step is to disconnect the ± 6 volt battery pack from the VCO, then the connector from the armored cable. This is necessary since any tools, watches, etc. that are carried near the sensor coil will cause a large signal that could damage the VCO if it was still operating.

d. The sensor site should be approached by following the armored cable, since this route avoids the poison oak that is throughout the area. The sensor container should be checked to insure that the top is high enough above ground level to prevent water from storms or melting snow from entering. After the cover is removed, a check for wildlife is recommended prior to attempting work. Once the sensor container is cleared and cleaned, the coil orientation should be verified. Next, the power cord is disconnected from the preamplifier, and the preamplifier batteries, which are located in another container buried approximately 15 feet south of the sensor, may then be

replaced. After utilizing the voltmeter to ascertain the proper polarity, the preamplifier is reconnected. Heating duct tape or one of a similar type should be used to seal the sensor container and plug any access holes.

e. The VCO may now be reconnected and powered. Head phones are then used to verify proper operation. If the VCO is operating satisfactorily, the VCO may be connected to the radio.

A complete set of back-up electronic components, a rechargeable soldering iron and spare connectors will repair most failures.

5. Gelyte Batteries

The batteries used to power the VCO and preamplifier are capable of numerous rechargings. Each battery is labeled and a record of chargings is maintained. The recommended charge procedure stipulates that both the 6 and 12 volt 18 ampere-hour-rated batteries should be charged at 1 ampere for approximately 20 hours for a full charge. Do not over-charge in excess of 24 hours more than the ampere-hour rating.

6. Radio Transmitter

Other than protection from water and dust, the only maintenance required on the MX320 radio is to insure the proper polarity of the power supply if it is disconnected and then reconnected and to attempt to maintain a constant voltage input below 8 volts dc.

B. BASE EQUIPMENT

1. Radio and Antenna

The Motorola base radio has no operator maintenance requirement. The only maintenance check for the receiving antenna is to be certain that there is adequate water protection at the connection between the antenna lead and the coaxial cable running to the base radio.

2. Hewlett-Packard 3900 Series Instrumentation Tape Recorder

The most important preventive maintenance considerations are: preventing oxide build-up in the transport tape path; keeping the recorder clean; and demagnetizing head and tape-path components. The main procedures are listed.

a. Tape Path Cleaning

Note: Do not use toluene or xylene cleaning agents on the pinchroller and do not allow cleaning agents to come in contact with the magnetic tape. Use cleaning agents sparingly and keep them out of bearings, especially at the base of the capstan.

All transport parts that come in contact with the tape require cleaning. Oxide build-up can cause degradation of high frequency response, distorted record and playback and tape and head damage. Worn tape heads cause changes in operational characteristics, too. Record sensitivity increases and there is a decrease in high-frequency response as the heads wear. The tape passing over the head presents

a relatively rough surface to the head. Since even high quality tapes will eventually cause wear on the heads, the only defense is to keep the tape-contacting components clean and as free of foreign matter as possible.

Clean tape heads with cotton-tipped applicators dampened in a head cleaner like DuPont Freon TF. Rotate the applicator against the head surface and note any discoloration of the cotton. Use as many applicators as required to avoid wiping the head surfaces with a dirty applicator. When the applicator comes away clean, the head surface is clean. Applicators should also be used to clean the tape guides, rollers, capstan and pinchroller. Take extra care to clean the undercut edges of the guides and roller grooves. Accumulations in the corners of the guides and roller grooves will damage the tape.

b. Demagnetizing Heads and Tape Path Components

The heads and tape path components should be demagnetized after every 72 hours of operation. To demagnetize:

1. Disconnect the power from the recorder.
2. Remove any tape on the recorder.
3. Remove the head cover and interhead shield.
4. Hold a bulk tape eraser as close as possible to the capstan assembly components.

5. Press and hold the "On" button and slowly rotate the bulk tape eraser in an arc over the capstan assembly components. Slowly draw the bulk tape eraser outward until at least two feet away, then release the "On" button.

6. Replace the interhead shield and head cover.

APPENDIX E: COMPUTER PROGRAMS

```

10 ! A DATA PLOTTING PROG
20 ! A$: TITLE
30 ! A1$: SUBTITLE
40 ! B$: X AXIS
50 ! C$: Y AXIS
60 ! P : THE PLOTTING PARAMS
70 !     0-X AXIS VALUES
80 !     1-AMB BINS
90 !     2-STEPS/CLASS
100 !     3-AVE AMB
110 !     4-% CLASSED
120 ! N9: # OF PTS - 1
130 ! N8: # OF PLOTS ON GRAPH
140 ! N5: # OF PLOTTING PARMETERS
150 ! Q$: AN ANSWER
160 ! Q0$: LOG PLOT ANSWER Y/N
170 ! L$: LOG SCALING FLAG
180 ! T$: TITLE FLAG
190 ! F1$: FLAG SIGNALS FIRST RUN
200 ! MISC: L1, L2, H1, H2, I, J, X, P1
210 ! Q, Q1, K2
220 ! A9$: AUTO MODE FLAG
230 !
240 !
250 !
260 !
270 !
280 REAL K1(8) ! LOG VALUES
290 SHORT D(200, 5) ! THE DATA
300 DIM A$(100), A1$(100), B$(100), C$(100), M9$(25)
310 T$="RESET"
320 CLEAR
330 F1$="RESET"
340 DISP "NOTE: ALWAYS ANSWER PROMPTS WITH"
350 DISP "'Y' OR 'N' FOR 'YES' OR 'NO'"

```

```

360 PLOTTER IS 705
370 GOSUB 550 ! READ DATA
380 GOSUB 850 ! SELECT&REV DATA
390 IF P1=0 THEN 4410 ! END PROG
400 IF P1=6 THEN 2480 ! REDRAW
410 IF A9$="SET" THEN 460
420 GOSUB 1380 ! INIT PLOT PARM
430 GOSUB 1770 ! DRAW AXES
440 GOSUB 2020 ! PLOT DATA
450 GOTO 380 ! MORE PLOTS?
460 GOSUB 4090 ! AUTO MODE
470 GOSUB 1770 ! DRAW AXES
480 GOSUB 2020 ! PLOT DATA
490 GOTO 380 ! RETURN FOR MORE
500 !
510 !
520 !
530 !
540 !
550 ! READ IN DATA
560 N8=1
570 N5=2
580 ! DISP "PLOTS/GRAPH"
590 ! INPUT N8
600 ! DISP "# PARMS PLOTTED"
610 ! INPUT N5
620 IF N5<5.5 THEN 650
630 DISP "TOO MANY, TRY AGAIN"
640 GOTO 600
650 DISP "DATA FILENAME"
660 INPUT F$
670 ASSIGN# 1 TO F$
680 N7=N8+1
690 READ# 1,1
700 N7=N7-1 ! SUB FOR MULTI READ

```

```

710 IF N7=0 THEN 680
720 READ# 1 : N9
730 N9=N9-1
740 FOR I=0 TO N9
750 FOR J=0 TO N5
760 READ# 1 : D(I,J)
770 NEXT J
780 NEXT I
790 RETURN
800 !
810 !
820 !
830 !
840 !
850 ! SELECT AND REVIEW DATA
860 CLEAR
870 DISP "CHOOSE PARAMETER"
880 DISP "      0-END PLOTTING"
890 DISP "      1-RAW DATA"
900 DISP "      2-PROCESSED"
910 ! DISP "      3-UNUSED"
920 ! DISP "      4-UNUSED"
930 ! DISP "      5-UNUSED"
940 DISP "      6-REPEAT PLOT"
950 INPUT P1
960 N6=N5+1
970 IF P1=6 THEN 1300
980 IF P1<=N6 THEN 1020
990 DISP "DATA NOT AVAILABLE"
1000 DISP "CHOOSE LOWER NUMBERED PARAMETER"
1010 GOTO 850
1020 F1$="SET"
1030 IF P1=0 THEN 1340
1040 P=P1
1050 A9$="RESET"

```

```

1060 L$="RESET"
1070 F1$="RESET"
1080 DISP "REVIEW"
1090 INPUT Q$
1100 IF Q$<>"Y" THEN 1300
1110 H1=D(0,0)
1120 H2=D(0,P)
1130 L1=D(0,0)
1140 L2=D(0,P)
1150 FOR I=0 TO N9 : FIND MAX/MIN
1160 H1=MAX(D(I,0),H1)
1170 L1=MIN(D(I,0),L1)
1180 H2=MAX(D(I,P),H2)
1190 L2=MIN(D(I,P),L2)
1200 DISP D(I,0),D(I,P)
1210 NEXT I
1220 DISP USING "3/"
1230 DISP "XMIN=";L1; "      XMAX=";H1
1240 DISP USING "3/"
1250 DISP "YMIN=";L2; "      YMAX=";H2
1260 DISP USING "3/"
1270 DISP "CONTINUE"
1280 INPUT Q$
1290 IF Q$<>"Y" THEN 870
1300 DISP "AUTOMODE"
1310 INPUT Q$
1320 IF Q$<>"Y" THEN 1340
1330 A9$="SET"
1340 RETURN
1350 !
1360 !
1370 !
1380 !
1390 ! INITIALIZE PLOT PARAMS
1400 DISP "INPUT XMIN,XMAX,YMIN,YMAX"

```



```

1410 INPUT X1,X2,Y1,Y2
1420 DISP "X AXIS LOG SCALE"
1430 DISP "ENTER Y OR N"
1440 INPUT Q0$
1450 IF Q0$<>"Y" THEN 1510
1460 X3=0
1470 X4=X1
1480 DISP "YINTV,YINTC"
1490 INPUT Y3,Y4
1500 GOTO 1530
1510 DISP "INPUT XINTV,YINTV,XINTC,YINTC"
1520 INPUT X3,Y3,X4,Y4
1530 I IF T$="SET" THEN REMEMBER TITLES
1540 IF T$="RESET" THEN GOSUB 1600 I ENTER TITLES
1550 RETURN
1560 I
1570 I
1580 I
1590 I
1600 I ENTER TITLE & X AXIS
1610 DISP "TITLE"
1620 INPUT A$
1630 DISP "SUBTITLE"
1640 INPUT A1$
1650 DISP "X AXIS TITLE"
1660 INPUT B$
1670 DISP "Y AXIS TITLE"
1680 INPUT C$
1690 IF N0>1.5 THEN GOSUB 3600 I ENTER PLOT TITLES
1700 T$="SET"
1710 RETURN
1720 I
1730 I
1740 I
1750 I

```

```

1760 !
1770 ! DRAW AXIES
1780 LOCATE 30, 110, 25, 85
1790 CSIZE 3
1800 ! DRAW LINEAR ?
1810 IF Q0$<>"Y" THEN GOSUB 2580
1820 ! OR DRAW SEMILOG
1830 IF Q0$="Y" THEN GOSUB 2770
1840 !
1850 ! PUT ON LABELS
1860 PLOT (X1+X2)/2, Y2+3*(Y2-Y1)/26, -2
1870 CSIZE 4
1880 LORG 6
1890 LABEL A$
1900 LABEL A1$
1910 PLOT (X1+X2)/2, Y1-(Y2-Y1)/8, -2
1920 LORG 4
1930 LABEL B$
1940 DEG
1950 LDIR 90
1960 LORG 6
1970 LORG 5
1980 PLOT X1-(X2-X1)/8, (Y1+Y2)/2, -2
1990 LABEL C$
2000 LDIR 0
2010 RETURN
2020 !
2030 !
2040 !
2050 !
2060 !
2070 ! MULTI PLOTS
2080 IF N7<>5 THEN 2120
2090 LINETYPE 4
2100 GOSUB 2310

```

```

2110 GOSUB 700
2120 IF N7<>4 THEN 2160
2130 LINETYPE 6
2140 GOSUB 2310
2150 GOSUB 700
2160 IF N7<>3 THEN 2200
2170 LINETYPE 7
2180 GOSUB 2310
2190 GOSUB 700
2200 IF N7<>2 THEN 2240
2210 LINETYPE 8
2220 GOSUB 2310
2230 GOSUB 700
2240 IF N7<>1 THEN 2280
2250 LINETYPE 1
2260 GOSUB 2310
2270 GOSUB 680
2280 IF N8=1 THEN RETURN
2290 GOSUB 3060 I THE PLOT TITLES
2300 RETURN
2310 I
2320 I
2330 I
2340 I PLOT DATA *****
2350 IF Q09<>"Y" THEN 2380
2360 MOVE LGT(D(0,0)),D(0,P)
2370 GOTO 2390
2380 MOVE D(0,0),D(0,P)
2390 FOR I=0 TO N9
2400 IF Q09<>"Y" THEN 2430
2410 PLOT LGT(D(I,0)),D(I,P)
2420 GOTO 2440
2430 PLOT D(I,0),D(I,P)
2440 NEXT I
2450 PENUP

```

```

2460 PENUP
2470 RETURN
2480 | FOR MORE GRAPHS
2490 GOSUB 1770 | DRAW AXIES
2500 GOSUB 2030
2510 GOTO 380
2520 |
2530 |
2540 |
2550 |
2560 |
2570 | DRAW LINEAR AXIES
2580 SCALE X1,X2,Y1,Y2
2590 AXES X3,Y3,X4,Y4
2600 LORG 5
2610 CSIZE 3.5
2620 FOR X=X1 TO X2 STEP X3
2630 PLOT X,Y1-(Y2-Y1)/55
2640 LABEL USING "K" , X
2650 NEXT X
2660 LORG 8
2670 FOR Y=Y1 TO Y2 STEP Y3
2680 PLOT X1-(X2-X1)/40,Y
2690 LABEL USING "K" , Y
2700 NEXT Y
2710 RETURN
2720 |
2730 |
2740 |
2750 |
2760 |
2770 | DRAWS A LOG X-AXIS
2780 | WITH LINEAR Y-AXIS
2790 LORG 8
2800 IF L$="SET" THEN 2840

```

```

2810 L$="SET"
2820 X1=LGT(X1)
2830 X2=LGT(X2)
2840 FOR I=0 TO 8
2850 K1(I)=LGT(I+2)
2860 NEXT I
2870 SCALE X1,X2,Y1,Y2
2880 MOVE X1,Y1
2890 DRAW X2,Y1
2900 FOR I=X1 TO X2
2910 MOVE I,Y1-(Y2-Y1)/55
2920 LABEL USING "K" ; 10*I
2930 FOR J=0 TO 8
2940 K2=K1(J)+I
2950 MOVE K2,Y1
2960 DRAW K2,Y1+(Y2-Y1)/100
2970 NEXT J
2980 NEXT I
2990 YAXIS X1,Y3
3000 LONG 8
3010 FOR Y=Y1 TO Y2 STEP Y3
3020 PLOT X1-(X2-X1)/40,Y
3030 LABEL USING "K" ; Y
3040 NEXT Y
3050 RETURN
3060 |
3070 |
3080 |
3090 |
3100 |
3110 | DRAW PLOT TITLES
3120 IF F1$="SET" THEN 3220
3130 DISP "START COORDS"
3140 INPUT C1,C2
3150 C3=C2

```

```

3160 C8=(X2-X1)/100
3170 C9=(Y2-Y1)/100
3180 MOVE C1*C8+X1, C2*C9+Y1
3190 DISP "POSIT OK"
3200 INPUT Q$
3210 IF Q$<>"Y" THEN 3110
3220 C2=C3
3230 MOVE (C1+10)*C8+X1, C2*C9+Y1
3240 CSIZE 3
3250 LORG 5
3260 LABEL M9$
3270 GOSUB 3570 I STEP DOWN
3280 IF N8=5 THEN 3320
3290 IF N8=4 THEN 3350
3300 IF N8=3 THEN 3380
3310 IF N8=2 THEN 3410
3320 LINETYPE 4
3330 LABEL M5$
3340 GOSUB 3490
3350 LINETYPE 6
3360 LABEL M4$
3370 GOSUB 3490
3380 LINETYPE 7
3390 LABEL M3$
3400 GOSUB 3490
3410 LINETYPE 8
3420 LABEL M2$
3430 GOSUB 3490
3440 LINETYPE 1
3450 LABEL M1$
3460 GOSUB 3490
3470 LINETYPE 1
3480 RETURN
3490 I
3500 I

```

```

3510 |
3520 |
3530 |
3540 | DRAW LINETYPE AND MOVE TO NEXT LABEL START
3550 MOVE (10+C1)*C8+X1,C2*C9+Y1
3560 DRAW (C1+25)*C8+X1,C2*C9+Y1
3570 C2=C2-5
3580 MOVE C1*C8+X1,C2*C9+Y1
3590 RETURN
3600 |
3610 |
3620 |
3630 |
3640 |
3650 |
3660 | ENTER PLOT TITLES
3670 IF N8<4.5 THEN 3700
3680 DISP "INPUT TITLE M5"
3690 M5$="RES = 100 HZ"
3700 IF N8<3.5 THEN 3730
3710 DISP "INPUT TITLE M4"
3720 M4$="RES = 75 HZ"
3730 IF N8<2.5 THEN 3760
3740 DISP "INPUT TITLE M3"
3750 M3$="RES = 50 HZ"
3760 IF N8<1.5 THEN 3790
3770 DISP "INPUT TITLE M2"
3780 M2$="RES = 25 HZ"
3790 DISP "INPUT TITLE M1"
3800 M1$="RES = 1 HZ"
3810 DISP "INPUT TITLE M9"
3820 M9$="PRF RESOLUTION"
3830 RETURN
3840 |
3850 |

```

```

3860 |
3870 |
3880 | THIS IS A TEST STUB
3890 | FOR THE TYPE BOX
3900 INPUT M9$
3910 DISP "ENTER M5$"
3920 INPUT M5$
3930 DISP "ENTER M4$"
3940 INPUT M4$
3950 DISP "ENTER M3$"
3960 INPUT M3$
3970 DISP "ENTER M2$"
3980 INPUT M2$
3990 DISP "ENTER M1$"
4000 INPUT M1$
4010 SCALE 0, 10, 0, 10
4020 X1=0
4030 X2=10
4040 Y1=0
4050 Y2=10
4060 F1$="RESET"
4070 GOSUB 3110
4080 GOTO 4080
4090 |
4100 |
4110 | THE AUTOMODE ROUTINE
4120 |
4130 CLEAR
4140 DISP
4150 DISP
4160 DISP "WELCOME TO AUTOMODE"
4170 DISP
4180 DISP "AUTOMODE INITIALIZES ALL "
4190 DISP "PLOTING PARAMETERS EXCEPT FOR"
4200 DISP "THE TITLE"

```



```

4210 INPUT A$
4220 X1=.01
4230 X2=100
4240 X3=0
4250 X4=X1
4260 Y1=-60
4270 Y2=0
4280 Y3=10
4290 Y4=-60
4300 Q0$="Y" | LOG FLAG
4310 B$="FREQUENCY (HZ)"
4320 C$="POWER DENSITY(dB)"
4330 IF P<>1 THEN 4350
4340 A1$=" "
4350 IF P<>2 THEN 4370
4360 A1$=""
4370 DISP "PUSH <END LINE> WHEN PLOTTER READY"
4380 BEEP
4390 INPUT Q$
4400 RETURN
4410 ASSIGN# 1 TO *
4420 DISP "BYE |"
4430 BEEP
4440 STOP
4450 PRINTER IS 703,60
4460 PRINT "&11140F", "&a5L", "&a200M"
4470 PPINT ""
4480 PRINT "'MIKPLT'-Houston 14 OCT 81", "

```

```

4490 PRINT
4500 PLIST 10, 4440
4510 STOP
4520 END

```

```

10 I PRINTER IS 703,60
20 I PRINT "&11L"
30 CLEAR
40 REAL D(200,3),T(199)
50 DISP "FILENAME? (6 OR LESS CHARACTERS)"
60 INPUT F$
70 CREATE F$,19
80 ASSIGN# 1 TO F$
90 ASSIGN# 2 TO "TRANS"
100 READ# 2, T0
110 ASSIGN# 2 TO *
120 DISP "TO GET OUT OF ENTER MODE, ENTER NEGATIVE FREQ
UENCY"
130 DISP
140 DISP "ENTER CONSTANT"
150 INPUT C
160 N0=0
170 DISP "ENTER FREQ, PARAM, DATA POINT=",N0
180 INPUT E(0),E(1)
190 IF E(0)<0 THEN 200
200 E(2)=-1+E(1)-T(N0)-C
210 FOR J=0 TO 2
220 D(N0,J)=E(J)
230 NEXT J
240 N0=N0+1
250 GOTO 170
260 DISP "DO YOU WANT TO EXAMINE DATA? (Y OR N)"
270 INPUT A$
280 IF A$="N" THEN 410
290 FOR I=0 TO N0
300 J=0
310 PRINT "D(",I,"0)=",D(I,0)," D(",I,"1)=",D(I,1),"
D(",I,"2)=",D(I,2)
320 NEXT I
330 DISP "DO YOU WANT TO CORRECT ANY ENTRIES? (Y OR N)"
340 INPUT B$
350 IF B$="N" THEN 410

```

```
360 DISP "TO CHANGE ANY ENTRIES TYPE IN D(I,J)=(NEW ENT  
RY) (CR), "  
370 DISP "WITH THE INDEXES I,J OF THE ENTRY YOU WANT TO  
CHANGE. "  
380 DISP "WHEN COMPLETED CHANGING AS MANY ENTRIES THAT  
YOU WANT HIT THE CONTINUE KEY"  
390 PAUSE  
400 GOTO 260  
410 PRINT# 1, N9  
420 FOR I=0 TO N9-1  
430 FOR J=0 TO 2  
440 PRINT# 1, D(I,J)  
450 NEXT J  
460 NEXT I  
470 ASSIGN# 1 TO *  
480 END
```

```

10 ! PRINTER IS 703,60
20 ! PRINT "&11L"
30 DIM T(199)
40 CLEAR
50 CREATE "TRANS",19
60 ASSIGN# 1 TO "TRANS"
70 DISP "THIS ALLOWS YOU TO ENTER TRANSFER FUNCTION DAT
A INTO A DATA FILE."
80 DISP " TO GET OUT OF ENTER MODE, ENTER 999"
90 N=0
100 DISP "ENTER VALUE N=",N
110 INPUT T(N)
120 IF T(N)=999 THEN 150
130 N=N+1
140 GOTO 100
150 DISP "DO YOU WANT TO EXAMINEDATA? (Y OR N)"
160 INPUT D$
170 IF D$="N" THEN 290
180 FOR I=0 TO N
190 PRINT "T(",I,")=";T(I)
200 NEXT I
210 DISP "DO YOU WANT TO CORRECT ANY ENTRIES? (Y OR N)"

220 INPUT C$
230 IF C$="N" THEN 290
240 DISP "TO CHANGE ANY ENTRIES TYPE IN T(I)=(NEW ENTRY
) (CR) "
250 DISP " WITH I BEING INDEX OF ENTRY YOU WANT TO CHAN
GE. "
260 DISP "WHEN COMPLETED HIT THE CONTINUE KEY. "
270 PAUSE
280 GOTO 150
290 PRINT# 1 , TO
300 ASSIGN# 1 TO *
310 END

```

BIBLIOGRAPHY

Barry, J. M., Power Spectra of Geomagnetic Fluctuations Between 0.1 and 10 Hz, M.S. Thesis, Naval Postgraduate School, Monterey, California 1978.

Beliveau, P. R., Telemetry Design for Solar Powered Geomagnetic Monitoring Station, M.S. Thesis, Naval Postgraduate School, Monterey, California 1980..

Campbell, W. H. and Matsushita, S., Physics of Geomagnetic Phenomena, v. 1, 2, Academic Press, 1967.

Clayton, W. F., Power Spectra of Geomagnetic Fluctuations Between 0.4 and 40 Hz, M.S. Thesis, Naval Postgraduate School, Monterey, California 1979.

Fraser-Smith, A. C. and Buxton, J. L., "Superconducting Magnetometer Measurements of Geomagnetic Activity in the 0.1 to 14 Hz Frequency Range", Journal of Geophysical Research, v. 80, No. 27, p. 3141-3147, August, 1975.

Jacobs, J. A., Geomagnetic Micropulsations, Springer, New York, 1970.

Kanamori, K., Takeuchi, H. and Uyeda, S., Debate About the Earth, Freeman Cooper and Company, 1970.

McDevitt, G. R. and Homan, B. B., Low Frequency Geomagnetic Fluctuations (.04 to 25 Hz) on Land and on the Floor of Monterey Bay, M.S. Thesis, Naval Postgraduate School, Monterey, California, 1980.

Polk, C. and Fitchen, F., "Schumann Resonances of the Earth-ionosphere Cavity - Extremely Low Frequency Reception at Kingston, R.I.", Res. Nat. Bur. Stand. Sect. D., v. 66, p. 313, 1962.

Santirocco, R. A. and Parker, D. C., "The Polarization and Power Spectrums of Pc Micropulsations in Bermuda", Journal of Geophysical Research, v. 68, p. 5545, 1963.

Wertz, R. and Campbell, W. H., "Integrated Power Spectra of Geomagnetic Field Variations with Periods of 0.3-300 s", Journal of Geophysical Research, v. 81, No. 28, p. 5131-5139, 1966.

INITIAL DISTRIBUTION LIST

	No. Copies
1. Defense Technical Information Center Cameron Station Alexandria, VA 22314	2
2. Library, Code 0142 Naval Postgraduate School Monterey, CA 93940	2
3. Department Chairman, Code 61 Department of Physics and Chemistry Naval Postgraduate School Monterey, CA 93940	1
4. Professor O. Heinz, Code 61Hz Department of Physics and Chemistry Naval Postgraduate School Monterey, CA 93940	2
5. Professor Paul H. Moose, Code 62Me Department of Electrical Engineering Naval Postgraduate School Monterey, CA 93940	2
6. CPT Michael W. Beard 300 West Broad Street Angola, IN 46703	2
7. Mr. William Audahazy Naval Ship Research & Development Center Annapolis Laboratory Annapolis, MD 21402	1
8. Chief of Naval Research Department of the Navy 800 North Quincy Street Arlington, VA 22217	
Code 100C1	1
Code 460	1
Code 464	3
Code 480	1
9. Commanding Officer Office of Naval Research Branch Office 1030 East Green Street Pasadena, CA 91106	1

10. Director 1
Naval Research Laboratory
Code 2627
Washington, D.C. 20350
11. Office of Research, Development, Test, 1
and Evaluation
Department of the Navy
Code NOP-987J
Washington, D.C. 20350
12. Air Force Office of Scientific Research 1
Department of the Air Force Directorate
of Physics (MPG)
Building 410
Bolling Air Force Base
Washington, D.C. 20332
13. Army Research Office 1
Department of the Army
Geosciences Division
Box 12211
Research Triangle Park, N.C. 27709
14. Deputy Under Secretary of the Army 1
for Operations Research
Room 2E261, Pentagon
Washington, D.C. 20310
15. LTC Larry L. Davis 2
Material & Safety Division
USANCA, Building 2073
7500 Backlick Road
Springfield, VA 22150